AMERICAN SOCIETY FOR MICROBIOLOGY | Antimicrobial Agents and Chemotherapy®

MECHANISMS OF ACTION: PHYSIOLOGICAL EFFECTS

New Insights into the Mechanism of Action of the Cyclopalladated Complex (CP2) in *Leishmania*: Calcium Dysregulation, Mitochondrial Dysfunction, and Cell Death

Angela M. A. Velásquez,[a,b] Paula J. Bartlett,[b] Irwin A. P. Linares,[c] Thais G. Passalacqua,[a] Daphne D. L. Teodoro,[a] Kely B. Imamura,[a] Stela Virgilio,[d] Luiz R. O. Tosi,[d] Aline de Lima Leite,[e] Marilia A. R. Buzalaf,[e] Jecika M. Velasques,[f] Adelino V. G. Netto,[f] Andrew P. Thomas,[b] Marcia A. S. Graminha[a]*

[a]São Paulo State University (Unesp), School of Pharmaceutical Sciences, Araraquara, São Paulo, Brazil
[b]Department of Pharmacology, Physiology, and Neuroscience, New Jersey Medical School, Rutgers, The State University of New Jersey, Newark, New Jersey, USA
[c]Department of Chemistry, São Carlos Institute of Chemistry–IQSC, University of São Paulo (USP), São Carlos, São Paulo, Brazil
[d]Department of Cellular and Molecular Biology and Pathogenic Bioagents, Ribeirão Preto Medical School, University of São Paulo, Ribeirão Preto, São Paulo, Brazil
[e]Laboratory of Biochemistry, Department of Biological Sciences, Bauru School of Dentistry, University of São Paulo (USP), Bauru, São Paulo, Brazil
[f]São Paulo State University (Unesp), Institute of Chemistry, Araraquara, São Paulo, Brazil

ABSTRACT The current treatment of leishmaniasis is based on a few drugs that present several drawbacks, such as high toxicity, difficult administration route, and low efficacy. These disadvantages raise the necessity to develop novel antileishmanial compounds allied with a comprehensive understanding of their mechanisms of action. Here, we elucidate the probable mechanism of action of the antileishmanial binuclear cyclopalladated complex $[Pd(dmba)(\mu\text{-}N_3)]_2$ (CP2) in *Leishmania amazonensis*. CP2 causes oxidative stress in the parasite, resulting in disruption of mitochondrial Ca^{2+} homeostasis, cell cycle arrest at the S-phase, increasing the reactive oxygen species (ROS) production and overexpression of stress-related and cell detoxification proteins, and collapsing the *Leishmania* mitochondrial membrane potential, and promotes apoptotic-like features in promastigotes, leading to necrosis, or directs programmed cell death (PCD)-committed cells toward necrotic-like destruction. Moreover, CP2 reduces the parasite load in both liver and spleen in *Leishmania infantum*-infected hamsters when treated for 15 days with 1.5 mg/kg body weight/day CP2, expanding its potential application in addition to the already known effectiveness on cutaneous leishmaniasis for the treatment of visceral leishmaniasis, showing the broad spectrum of action of this cyclopalladated complex. The data presented here bring new insights into the CP2 molecular mechanisms of action, assisting the promotion of its rational modification to improve both safety and efficacy.

KEYWORDS binuclear cyclopalladated complex, cutaneous leishmaniasis, leishmanicidal activity, necrotic death, calcium homeostasis, mitochondria, *Leishmania*

Leishmaniasis is a neglected parasitic disease caused by at least 20 species of the kinetoplastid genus *Leishmania* (1, 2) and is endemic in 98 countries (3). Cutaneous leishmaniasis (CL) is the most common clinical manifestation, while visceral leishmaniasis (VL) is a very severe systemic manifestation that can be fatal if left untreated (1, 2, 4). Causative CL species in the Old World are *L. tropica*, *L. major*, and *L. aethiopica*, in addition to *L. infantum* and *L. donovani*. In the Americas (New World), the species involved in CL are the *L. mexicana* species complex (especially *L. mexicana*, *L. amazonensis*, and *L. venezuelensis*) and the *Viannia* subgenus (most notably *L.* [*Viannia*] *braziliensis*, *L.* [*V.*] *panamensis*, *L.* [*V.*] *guyanensis*, and *L.* [*V.*] *peruviana*), in addition to *L. major*-like organisms and *L. chagasi*. For VL, the principal causative species of disease

Address correspondence to Marcia A. S. Graminha, marcia.graminha@unesp.br.

*Present address: Marcia A. S. Graminha, Departamento de Análises Clínicas–UNESP, Araraquara, São Paulo, Brazil.

Received 13 April 2021
Returned for modification 20 July 2021
Accepted 18 September 2021
Accepted manuscript posted online 11 October 2021
Published 18 January 2022

are the *L. donovani* species complex (i.e., *L. donovani* and *L. infantum* in the Old World, and *L. chagasi* in the New World) (5–7).

Available treatments for leishmaniasis have several limitations associated with high toxicity, difficult administration route, and low efficacy in areas of endemicity due to the emergence of resistant strains (4, 8–10). The adverse effects are mainly evident in leishmaniasis-HIV coinfection (1, 3). The current drugs for VL include pentavalent antimonials, amphotericin B (AmpB) and its lipid formulations (AmBisome), paromomycin, miltefosine, and drug combinations such as AmBisome/miltefosine, AmBisome/paromomycin, and miltefosine/paromomycin (2, 4, 11). For the CL, limited treatments are available (pentavalent antimonials, amphotericin B, and pentamidine) in comparison to VL, where these drugs are only recommended for the treatment of specific forms (2, 12). These challenges associated with just a few current pharmaceuticals highlight the urgent need to develop novel, safe, and effective leishmaniasis treatment drugs.

Thus, in order to contribute to new molecules that overcome the problems listed above, different strategies to identify new drugs against *Leishmania* spp. have been used (13–18). Many primary screenings of different compound libraries (natural products or synthetic molecules) have identified and validated hits (15, 19–32). Metal complexes with known antitumor bioactivity have been tested to treat various neglected diseases; some of them have exhibited antitrypanosomatid effects (21, 24–26, 28–30, 33–43). Moreover, the insertion of metal centers in antiparasitic drug structures is a strategy to increase their pharmacological activity by affecting multiple targets simultaneously (26). Au^{III} and Pd^{II} cyclometallated compounds and oxorhenium(V) complexes that inhibit different cysteine proteases of *Trypanosoma cruzi* and *Leishmania* spp. were developed as reported by Fricker and colleagues (25). Other authors reported the *in vitro* and *in vivo* leishmanicidal and trypanocidal activity of some Pd^{II} complexes (29, 30, 33, 35–38, 43–46). However, not all of these reports addressed the possible mechanism of action of these compounds. In general, studies involving Pd^{II} complexes reported that these compounds induce arrest of the cell cycle of parasites, generation of reactive oxygen species (ROS), interaction with DNA by electrostatic forces, irreversible inhibition of trypanothione reductase and cysteine protease, and inhibition of topoisomerase I (25, 30, 38, 43, 45, 46). The palladacycle compounds $[Pd_2Cl_2(C^2,N\text{-dmpa})_2(\mu\text{-dppe})]$ (DPPE 1.1) and $[Pd(C^2,N\text{-dmpa})(dppe)]Cl$ (DPPE 1.2), where dmpa is S(-)-*N*,*N*-dimethyl-1-phenethylamine and dppe is 1,2-bis(diphenylphosphino)ethane, reduced the parasite load of *L. amazonensis*-infected mice and reported cathepsin B and cysteine protease as their targets. However, the cell death mechanism induced by DPPE 1.1 and DPPE 1.2 has not been investigated (35–37). Other studies of DPPE 1.1 have described the cascade of effects produced after parasite treatment and showed that they also displayed action against other organisms (33, 34, 47). DPPE 1.1 exerts an apoptosis-like death in *T. cruzi* trypomastigotes and causes mitochondrion disruption (33); in *Paracoccidioides lutzii* and *Paracoccidioides brasiliensis*, the complex induced remarkable chromatin condensation, DNA degradation, superoxide anion production, metacaspase activity, and apoptosis- and autophagy-like mechanisms (34). In murine and cisplatin-resistant human tumor cells, DPPE 1.1 interacts with mitochondrial membrane thiol groups and induces the intrinsic apoptotic pathway (47).

Previously, we demonstrated that the binuclear cyclopalladated complex $[Pd(dmba)(\mu\text{-}N_3)]_2$ (CP2) delivers *in vivo* leishmanicidal activity in *L. amazonensis*-infected mice as a CL model via inhibition of DNA topoisomerase 1B (30). In this study, we identified the downstream effects of the *Leishmania* topoisomerase IB inhibition by CP2 and its probable mechanism of action against *L. amazonensis*. Here, we observed that CP2 increased ROS and cytosolic Ca^{2+} levels and collapsed the mitochondrial membrane potential, leading the parasite to promote necrosis or leading programmed cell death (PCD)-committed cells toward necrotic-like destruction. In addition, CP2 causes an alteration in the levels of translation, stress-response proteins, and ROS detoxification in *L. amazonensis*. Finally, we demonstrated that CP2 not only has *in vivo* leishmanicidal activity on a CL model but also displayed effective leishmanicidal activity

TABLE 1 Antileishmanial activity of CP2 against *Leishmania infantum* (IC_{50})[a]

Compound	*L. infantum* IC_{50} ± SD (SI)[b]	
	Promastigote	Amastigote
CP2	4.0 ± 0.4 (126.1)	4.7 ± 0.1 (107.6)
AmpB	0.9 ± 0.1 (25.1)	2.9 ± 0.1 (7.7)

[a]Data are the mean and standard deviation from three independent experiments. The results are expressed in μmol liter^{-1}.
[b]The selectivity index (SI, indicated in parentheses) was calculated as the CC_{50}/IC_{50} of CP2. $P < 0.05$ for all values.

against *L. infantum*-infected hamsters, a VL model, which demonstrates the widespread potential of this cyclopalladated complex.

RESULTS

CP2 displayed *in vitro* and *in vivo* antileishmanial activity against *L. infantum*. To evaluate the spectrum of action of CP2 beyond the effects previously reported (30), we analyzed the *in vitro* and *in vivo* efficacy of the compound using *L. infantum* as the causative agent of visceral leishmaniasis. CP2 displayed a high antileishmanial activity and selectivity index (SI) against both the insect promastigote stage (50% inhibitory concentration [IC_{50}], 4.0 μmol liter^{-1}; SI, 126.1) and the intracellular amastigote forms (IC_{50}, 4.7 μmol liter^{-1}; SI, 107.6) as reported in Table 1. The SI values were calculated using our previously reported values of cytotoxicity of CP2 against murine peritoneal macrophages (30).

L. infantum-infected golden hamsters were used as a VL model. The animals were treated for 15 days with CP2 (0.75 or 1.5 mg/kg body weight/day) or AmpB (20 mg/kg/day), and the parasite load of both spleen and liver was determined (Fig. 1). A dose of 1.5 mg/kg/day of CP2 caused an ~50% reduction in the parasite load of both liver and spleen similar to AmpB (at a dose 13-fold higher than CP2), without any alteration in biochemical markers of liver and kidney function (see Fig. S1 at http://hdl.handle.net/11449/214617), following previous work (30).

CP2 causes an alteration in the levels of stress-response proteins, protein translation, and ROS detoxification in *Leishmania*. Two-dimensional SDS-PAGE comparative analysis was performed to identify differentially expressed proteins in the presence or absence of CP2. *L. amazonensis* promastigotes at the logarithm growth phase were treated with 13.3 μmol liter^{-1} of CP2 for 72 h, a concentration corresponding to

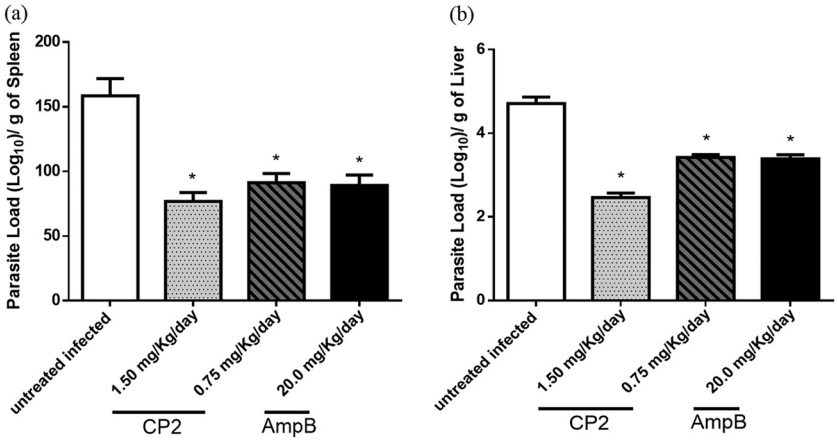

FIG 1 Parasite load of *L. infantum*-infected hamsters treated with CP2 or AmpB. Hamsters infected with *L. infantum* promastigotes in the stationary growth phase were treated with CP2 or AmpB commencing 75 days postinfection and lasting for 15 days. The parasite load was determined by the limiting dilution method at the end of the treatment in (a) the spleen and (b) the liver. The data are expressed as the mean ± standard deviation (SD). *, statistical significance of the difference relative to the untreated infected group ($P < 0.05$) was determined by ANOVA with Tukey's *post hoc* test.

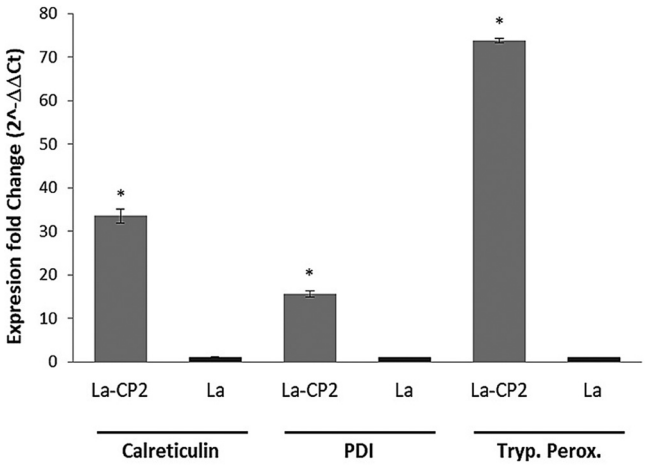

FIG 2 Relative gene expression of calreticulin, PDI, and tryparedoxin peroxidase of *Leishmania amazonensis* promastigotes after 72 h of exposure to CP2. The relative gene expression determined by RT-qPCR was calculated using the $2^{-\Delta\Delta CT}$ method, using kDNA mRNA expression as a reference and the *L. amazonensis* (La) in the absence of CP2 as the calibrator (see the supplemental material at http://hdl.handle.net/11449/214617). The data were expressed as the average ± SD. *, statistical significance of the difference relative to La in the absence of CP2, control ($P < 0.001$), was determined by ANOVA with Tukey's *post hoc* test. La-CP2 is the *L. amazonensis* treated with 13.3 μmol liter^{-1} CP2.

the previously determined IC_{50} value (30). The protein extracts obtained were separated by two-dimensional SDS-PAGE at a pH ranging from 4 to 7 (Fig. S2 at http://hdl.handle.net/11449/214617).

A total of 52 differentially expressed proteins identified through mass spectrometry analyses (Table S1 at http://hdl.handle.net/11449/214617) are related to chaperons/protein folding (48%), mitochondrial respiratory chain (17%), and ROS detoxification (14%), in addition to α- and β-tubulins. In order to minimize possible artifacts, the spots were selected after data filtration based on two factors, a *P* value of less than 0.5 with Student's *t* test comparing protein samples obtained in the presence or absence of CP2 and expression differences higher than 2-fold.

Among the overexpressed proteins, CP2 increased the levels of putative chaperons by at least 3-fold, including HSP70, LMXM_28_2770 (9-fold), two isoforms of putative calreticulin, LMXM_30_2600 (7-fold [pI 4.14] and 2-fold [pI 4.53]), and protein disulfide-isomerase (PDI), LMXM_36_6940 (3-fold). For the group of redox proteins, trypanothione reductase, LMXM_05_0350, and the peroxidoxin tryparedoxin peroxidase, LMXM_23_0040, increased by 6- and 4-fold, respectively.

Some proteins related to parasites' mitochondria were found overexpressed in the presence of CP2, such as mitochondrial cytochrome *c* oxidase subunit IV, LMXM_12_0670, and ribonucleoprotein p18, LMXM_15_0275, while others, such as putative mitochondrial chaperone heat shock 70-related protein 1 (mHSP70-1), LMXM_29_2550, were not expressed in the cells treated with CP2.

In the functional category of protein synthesis, the putative translation elongation factor 1-beta, LMXM_33_0840, was 11-fold higher than that of to the control, while the elongation factor 1-alpha, LMXM_17_0080, the elongation factor 2, LMXM_36_0180, and the 60S acidic ribosomal protein P0, LMXM_27_1380, were only expressed in the absence of CP2. The putative carboxypeptidase, LMXM_32_2540, in the category of amino acid metabolism, was increased 2-fold. Additionally, reverse transcriptase quantitative PCR (RT-qPCR) data also show a correspondence between transcriptional and protein levels for calreticulin, PDI, and tryparedoxin peroxidase (Fig. S3 at http://hdl.handle.net/11449/214617) induced by CP2 (Fig. 2).

CP2 arrests cell cycle progression at S-phase in *Leishmania*. Previously, we demonstrated that CP2 inhibited the cleavage step of DNA topoisomerase 1B of *Leishmania*

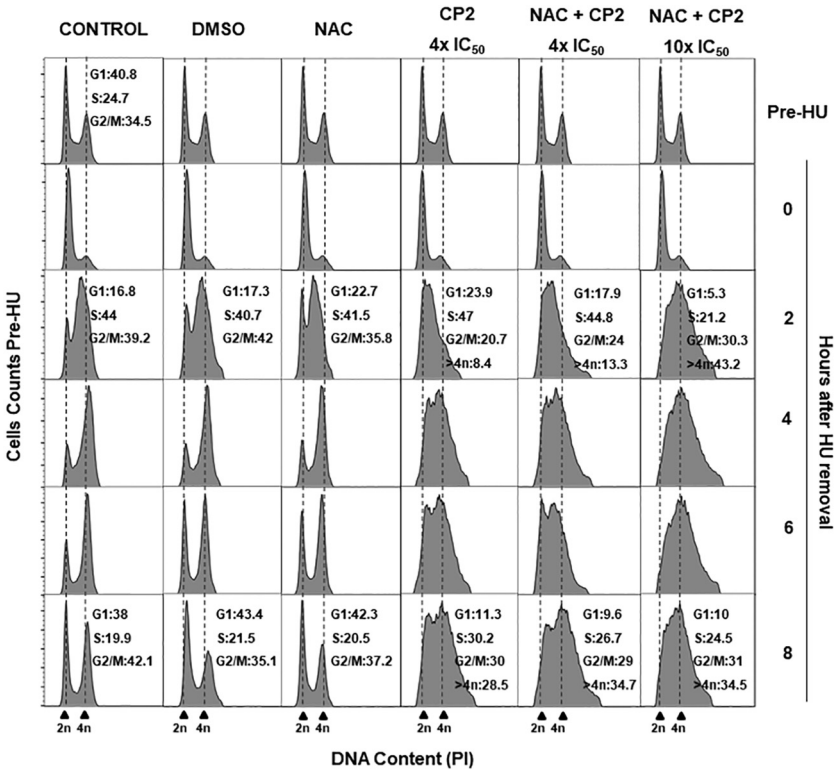

FIG 3 CP2 effect on the cell cycle of *Leishmania amazonensis*. Promastigotes in the mid-log growth phase were synchronized by adding 5 mmol liter^{-1} HU for 8 h and then transferred to an HU-free medium containing 0.03% DMSO (control). The parasites were treated with CP2 (4× IC_{50}, 53.2 μmol liter^{-1}), 20 μmol liter^{-1} NAC or CP2 (4× IC_{50}, 53.2 μmol liter^{-1} or 10× IC_{50}, 133 μmol liter^{-1}) plus 20 μmol liter^{-1} NAC. Cells were collected at 0, 2, 4, 6, and 8 h, and the DNA content was measured by flow cytometry. Each histogram represents the data of 50,000 events; 2n and 4n indicate nonreplicated and replicated DNA, respectively. The percentage of cells in G_1, S, and G_2/M phases is indicated for cells before treatment with HU (pre-HU) and at 2 h and 8 h after the removal of HU. HU, hydroxyurea; NAC, N-acetyl-L-cysteine. $P < 0.01$.

(30), leading to the accumulation of DNA damage and arrest in the cell cycle progression. To investigate the effect of CP2 on cell cycle progression, hydroxyurea (HU)-synchronized *L. amazonensis* promastigotes were treated with CP2 or CP2 plus the ROS inhibitor N-acetyl L-cysteine (NAC), and the progression of the cell cycle was followed by determining the parasite DNA content by flow cytometry (Fig. 3).

The data obtained demonstrate that CP2 induced the accumulation of a higher proportion of cells in the S-phase, indicating an arrest of the cell cycle at this phase after CP2 treatment at 53.2 μmol liter^{-1}. Notably, this effect is not abolished by the addition of NAC. Moreover, promastigotes in the presence of 133 μmol liter^{-1} CP2 (10× IC_{50}) increased the proportion of cells with 4n (see Fig. 3) DNA content, indicating that the effect of CP2 on the parasite cell cycle progression occurred independently of ROS.

CP2 increases ROS levels in *Leishmania*. Promastigotes were exposed for 60 min to different concentrations of CP2 to determine its ability to increase cellular ROS levels every 5 min. CP2 increased ROS production in a dose-dependent manner (Fig. 4). This finding correlates with the proteomic data that showed overexpression of trypanothione reductase, peroxiredoxin, and tryparedoxin peroxidase, enzymes involved in the trypanothione-mediated hydroperoxide metabolism for detoxification of endogenous or exogenous oxidative agents (48).

CP2 disrupts Ca^{2+} homeostasis in *Leishmania* in a dose-dependent manner. Considering that oxidative stress is often associated with a rise in intracellular Ca^{2+} concentration ($[Ca^{2+}]_i$) (49–52), we determined the effect of CP2 on $[Ca^{2+}]_i$ in single-promastigote cells by live-cell fluorescence imaging using the ratiometric Ca^{2+}

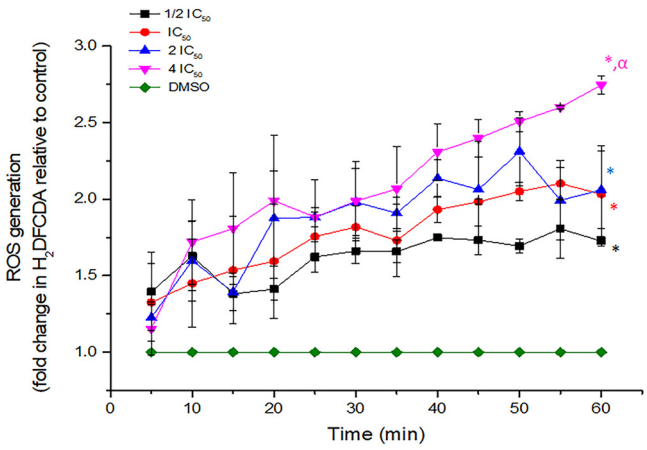

FIG 4 CP2-dependent ROS generation in *L. amazonensis*. Promastigote forms of *L. amazonensis* were treated with CP2 (0.5× IC_{50}, 6.7 μmol liter^{-1}; IC_{50}, 13.3 μmol liter^{-1}; 2× IC_{50}, 26.6 μmol liter^{-1} and 4× IC_{50}, 53.2 μmol liter^{-1}) for 60 min. ROS generation was measured spectrofluorimetrically using the probe H_2DFCDA. The parasites were treated with 0.1% DMSO as a control. Data are the mean ± SD from three independent experiments. *, statistically significant difference relative to DMSO control ($P < 0.001$); α, statistically significant difference relative to parasites treated with 0.5× IC_{50} of CP2 ($P < 0.01$). Statistical significance was determined by ANOVA with Student-Newman-Keuls multiple-comparison test.

indicator Fura-2/AM (Fig. 5). After CP2 addition, increases in $[Ca^{2+}]_i$ were observed in the majority of cells after a delay of 5 to 10 min. The subsequent addition of the Ca^{2+} ionophore ionomycin increased $[Ca^{2+}]_i$ to the maximum, and this occurred with no delay. The presence of an ionomycin response and maintenance of the Fura-2 dye load of the cells was used to validate that the cells remained viable during the experiment. The $[Ca^{2+}]_i$ responses to CP2 varied in magnitude, with an increase to near-maximal $[Ca^{2+}]_i$ levels (relative to the ionomycin response) in some promastigotes (Fig. 5a). In contrast, others exhibited small peaks and only partial increases in $[Ca^{2+}]_i$ (Fig. 5b). When the responses were averaged from all parasites in the imaging field, the profile $[Ca^{2+}]_i$ showed a progressive increase during the incubation period (Fig. 5c). Additionally, the percentage of parasites that exhibited changes in $[Ca^{2+}]_i$ during the incubation period with CP2 increased in a dose-dependent manner (Fig. 5d). In the presence of 3.8 μmol liter^{-1}, an increase in $[Ca^{2+}]_i$ was detected in 20% of cells during the 25 to 30 min time course of the experiment, whereas in the presence of 7.5 μmol liter^{-1} and 15 μmol liter^{-1} responses were detected in 60% and 98% of cells, respectively. Following the large $[Ca^{2+}]_i$ increase during continuing incubation with high doses of CP2, some cells showed a loss of the total Fura-2 signal, which was taken as an indicator of cell death (Fig. S4 at http://hdl.handle.net/11449/214617). Thus, the increase in Ca^{2+} levels appears to presage cell death in response to CP2 (Fig. 5c).

Removal of extracellular Ca^{2+} did not affect the percentage of promastigotes of *L. mexicana* exposed to CP2, in which increases in $[Ca^{2+}]_i$ were observed (Fig. 6a and b). These data show that CP2-induced $[Ca^{2+}]_i$ responses are observed in the absence of extracellular Ca^{2+}, indicating that the observed $[Ca^{2+}]_i$ increase is caused by Ca^{2+} release from an intracellular Ca^{2+} store, such as the endoplasmic reticulum (ER), acidic compartments, or mitochondria. Of note, an increase in dead cells after CP2 addition was also still observed in the absence of extracellular Ca^{2+} (Fig. 6c).

The metal chelator TPEN does not suppress the CP2-dependent $[Ca^{2+}]_i$ response. Since CP2 is a complex of Pd^{2+}, and heavy metals can affect Ca^{2+} channels and pumps, we tested the effect of TPEN (*N*,*N*,*N*′,*N*′-tetrakis [2-pyridylmethyl] ethylenediamine), a permeable cell and highly selective heavy metal-chelating agent with low affinity for Mg^{2+} and Ca^{2+} (53, 54). *L. mexicana* promastigotes were exposed to 10 μmol liter^{-1} TPEN followed by CP2 addition (3.8 and 7.5 μmol liter^{-1}) (Fig. 7). It was observed that TPEN does not inhibit the ability of CP2 to mobilize intracellular Ca^{2+}

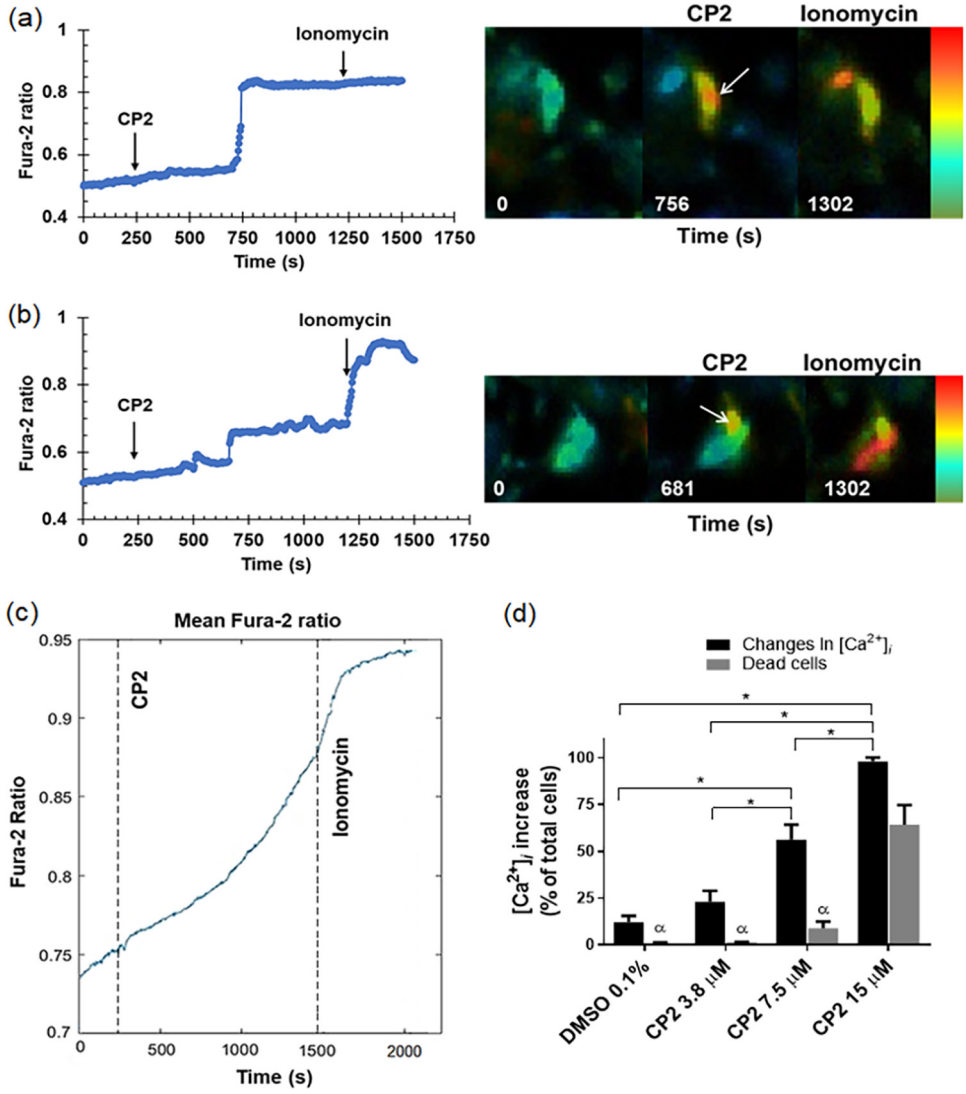

FIG 5 Effect of CP2 on the $[Ca^{2+}]_i$ of *Leishmania mexicana* promastigotes. The parasites were cultivated until the mid-log growth phase and then loaded with 5 μmol liter^{-1} Fura-2/AM in a loading buffer containing 1.3 mmol liter^{-1} of $CaCl_2$. Changes in $[Ca^{2+}]_i$ were measured with Fura-2 excitation at 340/380 nm and emission at >510 nm and are plotted as the 340/380 ratio (Fura-2 ratio). (a and b) Representative single-cell traces of large (a) and small (b) $[Ca^{2+}]_i$ changes in response to 7.5 μmol liter^{-1} CP2 treatment of promastigotes are shown. Ionomycin (10 μmol liter^{-1}) was added at the end of each experiment to determine the maximal $[Ca^{2+}]_i$ response for each cell. The right panels shows pseudocolor images demonstrating the increase in fluorescence ratio related to an increase in $[Ca^{2+}]_i$ from blue (lowest ratio) to red (highest ratio) in the absence and presence of drugs. (c) Averaged trace for 100 cells in the imaging field. (d) Mean percentage of parasites with a change in $[Ca^{2+}]_i$ in the presence of 3.8, 7.5, or 15 μmol liter^{-1} CP2; 0.1% DMSO was used as a control. Cell death counts reflect cells that showed total loss of Fura-2 by the end of the imaging experiment. Summary data are the mean ± SD from three independent experiments. α, statistically significant difference relative to dead cells in the presence of 15 μmol liter^{-1} CP2; *, statistically significant difference between groups ($P < 0.001$) was determined by two-way ANOVA followed by Tukey's multiple-comparison test.

(Fig. 7a and b). CP2 (7.5 μmol liter^{-1})-induced $[Ca^{2+}]_i$ responses were observed in ~60% of cells in the presence or absence of TPEN (Fig. 7c). Heavy metals have been shown to alter the fluorescent properties of Ca^{2+} indicator dyes (53). The addition of CP2 does not alter the fluorescence of Fura-2 in *Leishmania*, and TPEN does not perturb the Ca^{2+} response to this agent, which indicates that Pd^{2+} is coordinated with *N*,*N*-dimethylbenzylamine (dmba), and azide (N_3–) in the active species of CP2, which contributes to its effect on $[Ca^{2+}]_i$ mobilization. Notably, the dmba by itself did not exhibit

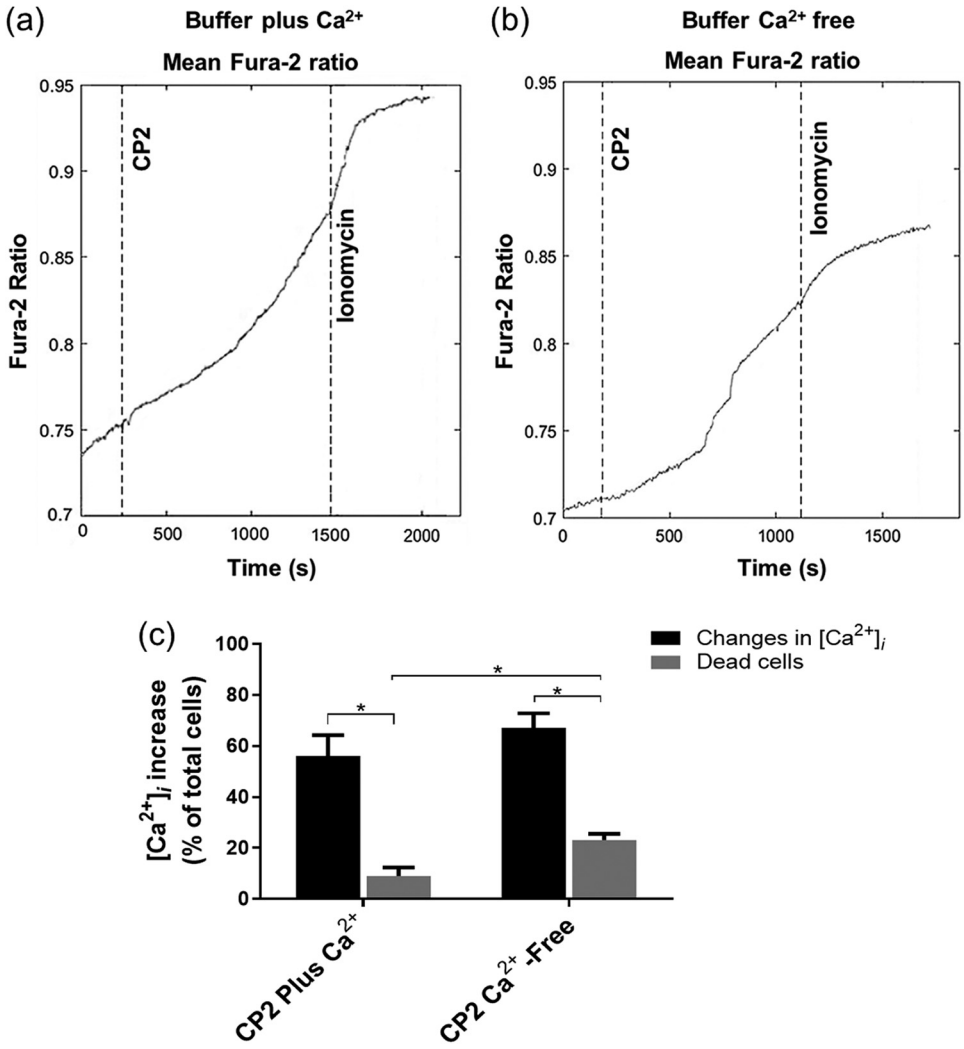

FIG 6 Removal of extracellular Ca^{2+} does not perturb CP2-induced $[Ca^{2+}]_i$ responses in *Leishmania mexicana*. (a and b) A representative experiment of promastigotes cultivated until the mid-log growth phase and then loaded with Fura-2/AM in a loading buffer with (a) or without (b) 1.3 mmol liter^{-1} of $CaCl_2$ and treated with 7.5 μmol liter^{-1} CP2 followed by 10 μmol liter^{-1} ionomycin. Traces averaged from 100 individual parasites. (c) Mean of the percentage of parasites with an increase in $[Ca^{2+}]_i$ and the percentage of dead cells in the presence or absence of extracellular Ca^{2+} after CP2 addition. Summary data are the mean ± SD from three independent experiments. *, statistically significant difference between groups ($P < 0.001$) was determined by two-way ANOVA followed by Tukey's multiple-comparison test.

leishmanicidal activity, as previously demonstrated (29). Nevertheless, it cannot be ruled out that CP2 can participate in competing ligand exchange reactions with other molecules or bridge splitting reactions during the experiments, affording new species, which may be responsible for the observed activity.

CP2 induces Ca^{2+} release from mitochondria but not ER or acidic Ca^{2+} pools in *Leishmania*. Fura-2/AM-loaded promastigotes in the presence of extracellular Ca^{2+} were exposed to nigericin (55) or cyclopiazonic acid (CPA) (56), followed by the addition of CP2 in order to determine the Ca^{2+} store targeted by CP2. The addition of nigericin, which releases Ca^{2+} from acidic compartments such as the acidocalcisome and acidic vesicles, resulted in an elevation of $[Ca^{2+}]_i$ in ~60% of the parasites. Nevertheless, an increase in $[Ca^{2+}]_i$ was still observed after adding CP2 to nigericin-treated cells in 90% of the cells. Also, in cells, that responded to nigericin, an additional increase in response to CP2 was observed in ~77% (Fig. 8a and b). Thus, CP2 does not act by mobilizing Ca^{2+} from acidic pools in *Leishmania*.

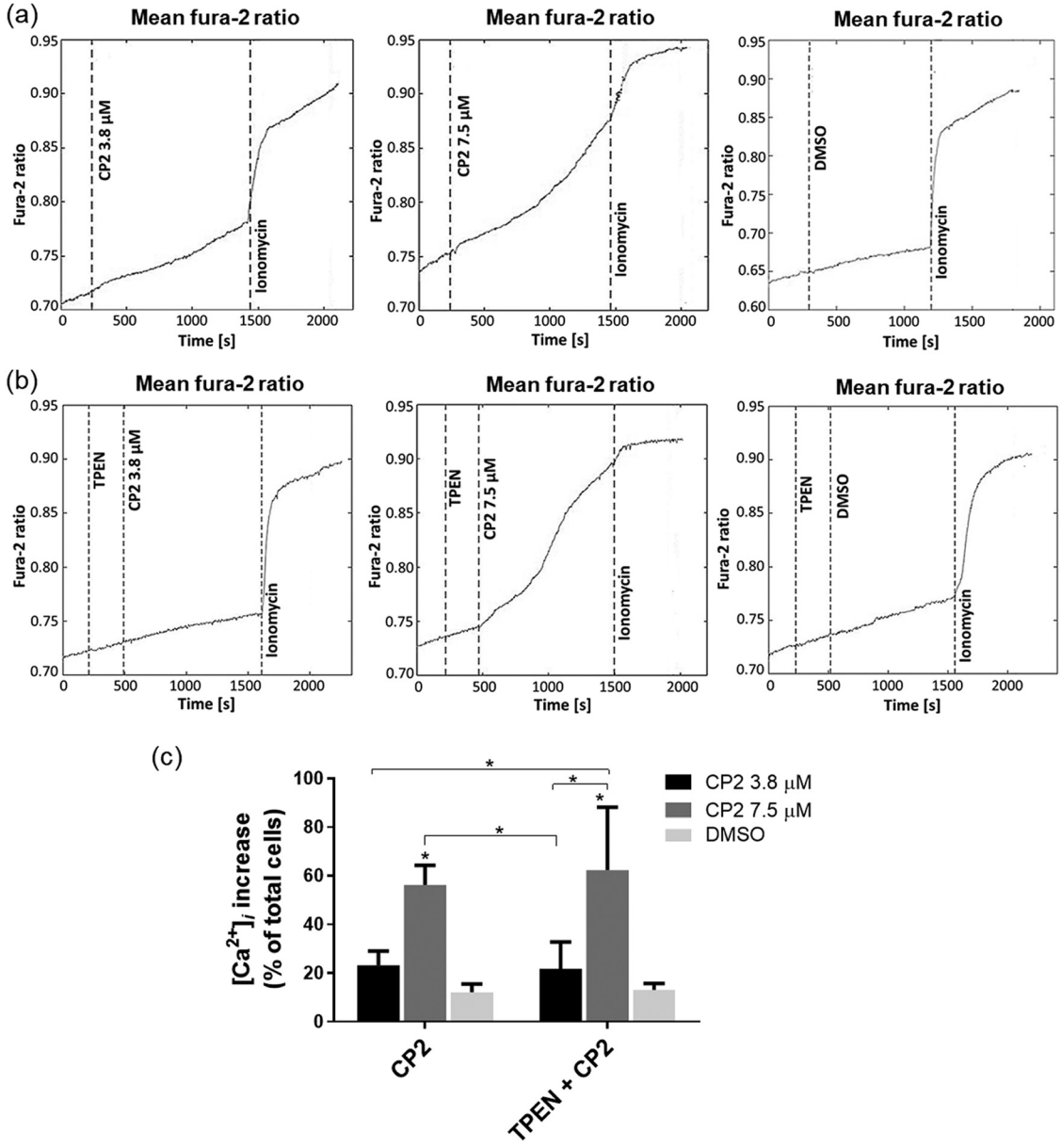

FIG 7 Effect of CP2 on the *L. mexicana* $[Ca^{2+}]_i$ in the presence of TPEN, a heavy metal chelating agent. (a) Representative experiment of promastigotes treated with 3.8 or 7.5 μmol liter^{-1} CP2 followed by 10 μmol liter^{-1} ionomycin; (b) promastigotes treated with 10 μmol liter^{-1} TPEN plus 3.8 or 7.5 μmol liter^{-1} CP2, followed by 10 μmol liter^{-1} ionomycin. Each trace is the average from at least 100 individual parasites. (c) Summary data of the percentage of cells with increased $[Ca^{2+}]_i$; 0.1% DMSO was used as a control. Data are the mean ± SD from three independent experiments. *, statistically significant difference relative to DMSO control ($P < 0.001$) was determined by two-way ANOVA followed by Tukey's multiple-comparison test.

CPA, a specific inhibitor of the sarco-endoplasmic reticulum Ca^{2+}-ATPase (SERCA) (56), was used to investigate whether CP2 releases Ca^{2+} from the ER. Ca^{2+} responses in Fura-2-loaded parasites were observed after the addition of both CPA and CP2, suggesting that the release of Ca^{2+} caused by these two drugs is independent (Fig. 9a). Almost 60% of the parasites showed an increase in $[Ca^{2+}]_i$ in response to CPA, and 90% gave an $[Ca^{2+}]_i$ increase upon subsequent CP2 addition. The percentage of cells that responded to both CPA and CP2 was ~70% (Fig. 9b).

The results described above indicate that the CP2-dependent elevation of intracellular Ca^{2+} is not due to release from acidocalcisomes or the ER. To determine whether mitochondria might be the Ca^{2+} source, promastigotes were exposed to CP2 and the

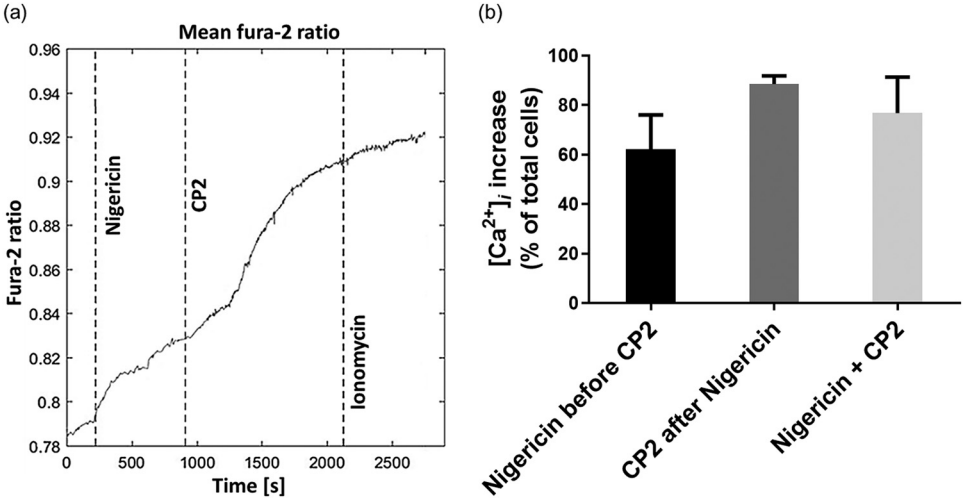

FIG 8 Effects of CP2 on $[Ca^{2+}]_i$ in *Leishmania mexicana* after the addition of nigericin. (a) Representative experiment of promastigotes treated with 2.5 μmol liter^{-1} nigericin, followed by 7.5 μmol liter^{-1} CP2 and 10 μmol liter^{-1} ionomycin. The trace shows an average of at least 100 individual parasites. (b) Mean percentage of parasites with a change in $[Ca^{2+}]_i$ in the presence of nigericin, subsequent CP2 addition, and those that responded to both nigericin and CP2. Data are the mean ± SD from three independent experiments. There are no statistically significant differences between groups determined by the one-way ANOVA multiple-comparison test ($P < 0.05$).

mitochondrial uncoupler FCCP (Fig. 10). The cell percentage with a $[Ca^{2+}]_i$ increase in response to CP2 was significantly decreased to about 10% by the pretreatment with FCCP (Fig. 10b). Similarly, prior treatment with CP2 decreased the response to subsequent FCCP addition. In both sequential addition paradigms, the percentage of parasites that responded to both FCCP and CP2 was only ~5% (addition of FCCP followed by CP2 or CP2 followed by FCCP). Thus, these data suggest that CP2 mobilizes Ca^{2+} from a mitochondrial pool.

CP2 depolarized the mitochondrial membrane potential of *Leishmania*. To investigate whether CP2 alters the mitochondrial membrane potential ($\Delta\psi_m$) of *L.*

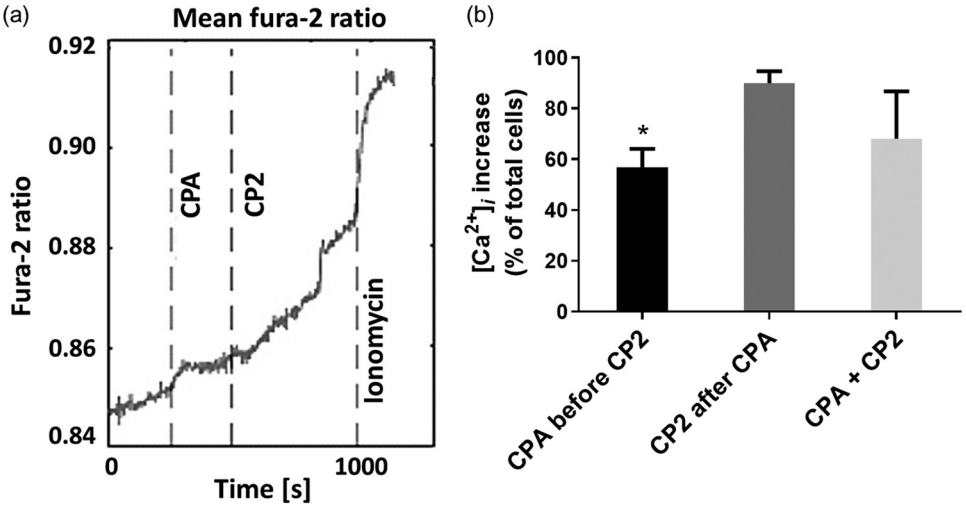

FIG 9 Effects of CP2 on $[Ca^{2+}]_i$ in *Leishmania mexicana* after the addition of cyclopiazonic acid (CPA). (a) Representative experiment of promastigotes treated with 10 μmol liter^{-1} CPA, followed by 7.5 μmol liter^{-1} CP2 and 10 μmol liter^{-1} ionomycin. The trace shows an average of at least 100 individual parasites. (b) Mean of the percentage of parasites with increases in $[Ca^{2+}]_i$ in the presence of CPA, subsequent addition of CP2, and those that respond to both CPA and CP2. Data are the mean ± SD from three independent experiments. *, statistically significant differences relative to CP2 after CPA addition ($P < 0.05$) were determined by one-way ANOVA multiple-comparison test.

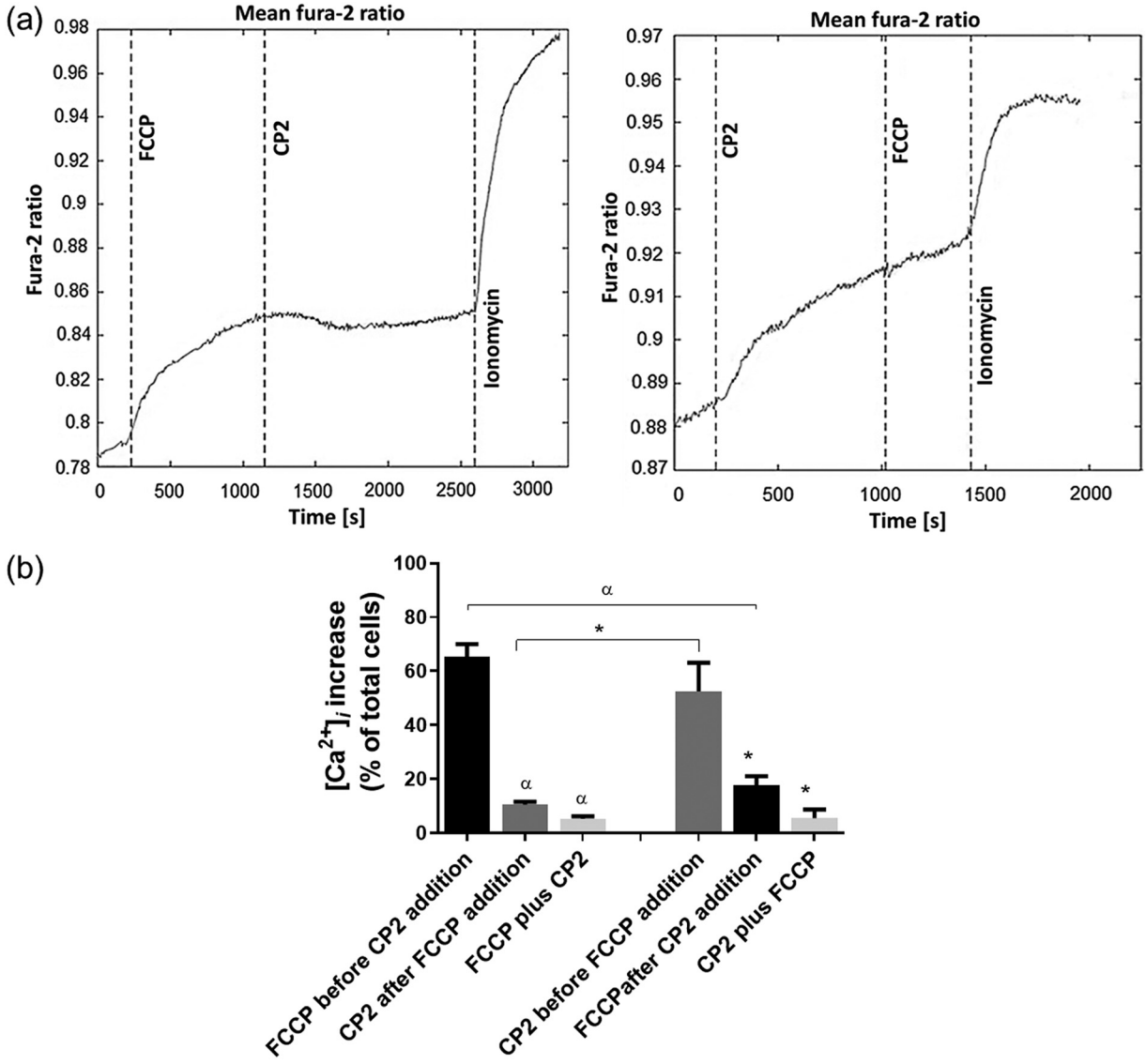

FIG 10 Effect of CP2 on the *Leishmania mexicana* $[Ca^{2+}]_i$ before or after addition of FCCP (mitochondrial uncoupler). (a) Representative experiment of promastigotes treated with FCCP followed by CP2 (5 μmol liter^{-1} and 7.5 μmol liter^{-1}, respectively) or CP2 followed by FCCP (7.5 μmol liter^{-1} and 5 μmol liter^{-1}, respectively) and ionomycin (10 μmol liter^{-1}). Each trace is the average from at least 100 individual parasites. (b) Summary data showing the mean ± SD from three independent experiments. *, statistically significant difference relative to cells with $[Ca^{2+}]_i$ increase in the presence of CP2 ($P < 0.05$); α, statistically significant difference relative to cells with $[Ca^{2+}]_i$ increase in the presence of FCCP ($P < 0.001$) were determined by two-way ANOVA followed by Tukey's multiple-comparison test.

amazonensis, promastigotes were exposed to different concentrations of CP2 based on the IC_{50} value for *L. amazonensis* previously determined (30) (IC_{50}, 13.3 μmol liter^{-1} and 2× IC_{50}, 26.6 μmol liter^{-1}) for 60 min, and changes in $\Delta\psi_m$ were determined with JC-1. The spectrofluorometric data (Fig. 11) showed a decrease in the relative fluorescence intensity in all tested concentrations, indicating the membrane potential's depolarization. Moreover, at a dose of 26.6 μmol liter^{-1} of CP2, the decrease in the relative fluorescence intensity was similar to that caused by the mitochondrial uncoupler CCCP.

CP2 causes necrotic parasite death. The cell death mechanism induced by CP2 was investigated using a dual acridine orange (AO)/ethidium bromide (EB) staining method (Fig. 12) (57). Cultures of *L. amazonensis* promastigotes were exposed to CP2 for 6, 24, or 48 h, 200 parasites of each sample were analyzed, and the percentages of viable cells (green), apoptotic-like cells (orange), or necrotic cells (red) were calculated

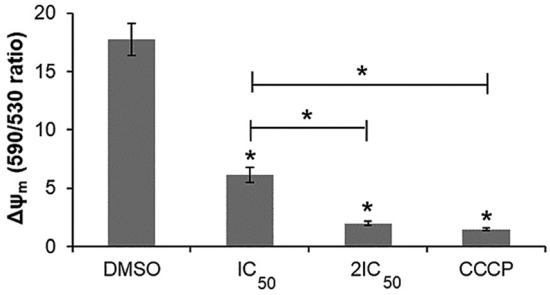

FIG 11 Analysis of the mitochondrial membrane potential $\Delta\psi_m$ of *L. amazonensis* promastigotes. Promastigotes (2×10^6/ml) were incubated with the potential-sensitive probe JC-1 (10 μmol liter^{-1}) for 10 min after exposure to different doses of CP2 (IC_{50}, 13.3 μmol liter^{-1}; $2\times$ IC_{50}, 26.6 μmol liter^{-1}) for 60 min or CCCP (50 μmol liter^{-1}) 15 min before the addition of JC-1. For the untreated controls, promastigotes were incubated in the presence of 0.1% DMSO. Dose-dependent changes in relative $\Delta\psi_m$ values were expressed as the fluorescence ratio at 590 nm/530 nm. *, statistically significant difference relative to the control and between groups ($P < 0.001$). Statistical analysis was determined by ANOVA followed by Student-Newman-Keuls multiple-comparison test.

(Fig. 12b to d). It was observed that 6 h post-CP2-treatment (Fig. 12b), promastigotes presented mainly apoptotic-like features (~40%). However, exposure to CP2 for more extended periods (24 h and 48 h) produced ~50% and 58% necrotic cells, respectively (Fig. 12c and d). Cell viability was significantly improved by NAC pretreatment, resulting in the prevention of apoptotic-like and necrotic cells (Fig. 12b to d). These data suggest that CP2-induced ROS formation triggers a programmed cell death response.

DISCUSSION

We previously reported that the cyclopalladated complex CP2 inhibits *Leishmania* topoisomerase IB (30), which might lead to DNA damage, triggering cell cycle arrest and DNA repair (58–60). Here, we demonstrated that although CP2 is a ROS-inducing compound, the observed cell cycle arrest in S-phase, but not cell death, is ROS-independent, unlike DNA damage effects in *Trypanosoma brucei*, which are ROS inducible (61). Moreover, cells that have sustained DNA damage activate repair proteins, which cause NAD depletion and glycolysis inhibition. As a result, cells that become quickly depleted of ATP suffer necrotic cell death (62). Thus, we hypothesized that CP2 is causing several and simultaneous deleterious effects on the parasite.

Some cyclopalladated compounds act by targeting mitochondria (33, 34, 47, 63). This kind of compound could interact with thiol groups of mitochondrial membrane proteins, causing dissipation of the mitochondrial membrane potential, uncoupling of oxidative phosphorylation, increasing cytosolic Ca^{2+} and decreasing ATP levels, which lead to apoptosis, as reported by Serrano and colleagues (47). In this study, we demonstrated that CP2 increased ROS and cytosolic Ca^{2+} levels in *Leishmania*.

The trypanosomatid mitochondrion is a major source of ROS (64), and in order to deal with oxidative stress, the parasite produces several antioxidant molecules, including glutathione/trypanothione (64–66). Our proteomic analyses revealed other important overexpressed components, such as trypanothione reductase and tryparedoxin peroxidase induced by CP2. The trypanothione system is unique in trypanosomatids and protects them from oxidative damage and toxic heavy metals (67, 68). The combined action of trypanothione reductase, tryparedoxin, and tryparedoxin peroxidase is central to the maintenance of hydroperoxide metabolism (69). The trypanothione system is related to the mode of action and resistance to drugs containing metals, such as antimonials, by decreasing its thiol buffering capacity in *Leishmania* (68). In addition, elevated ROS levels are associated with an increase in peroxiredoxins involved in peroxynitrite protection (70). Thus, high peroxiredoxin levels observed in *Leishmania* after CP2 exposure might be related to the cell's attempt to stabilize the mitochondrial

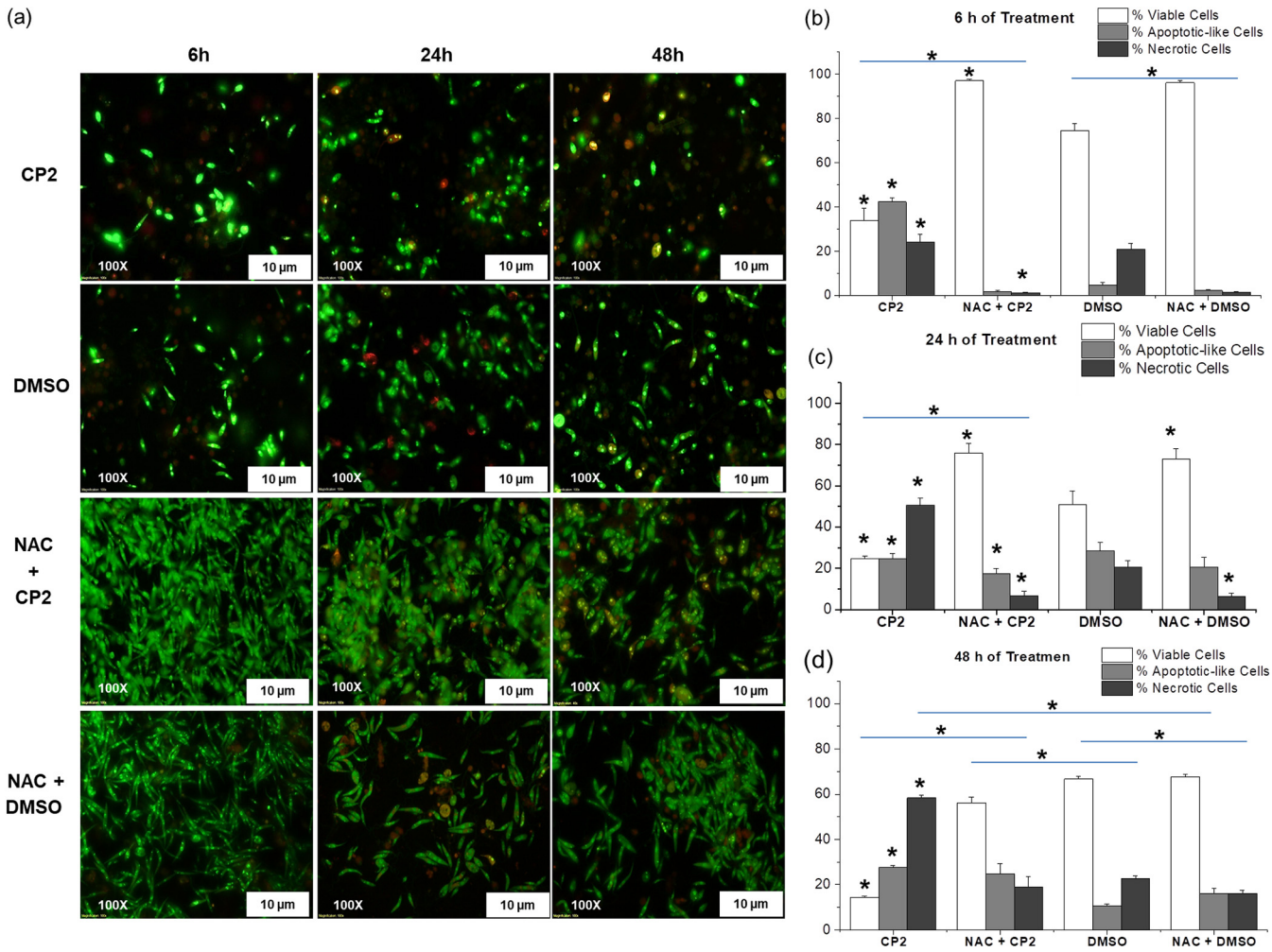

FIG 12 CP2-induced necrotic cell death in *L. amazonensis*. Promastigotes were treated with 13.3 μmol liter^{-1} CP2 for 6, 24, and 48 h in the presence and absence of 20 μmol liter^{-1} NAC pretreatment for 2 h. The parasites were stained with acridine orange and ethidium bromide (AO/EB) and immobilized to be analyzed under a fluorescence microscope (Axio Imager A2; Zeiss), at $\times$100 magnification. (a) Staining of necrotic/apoptotic-like *L. amazonensis* promastigotes with AO/EB, where viable cells are green, necrotic cells red, and apoptotic-like cells yellow-orange. The images were captured with an Axio Cam MRm camera and processed using AxioVision software. (b to d) A total of 200 parasites from each sample were evaluated to determine the number of necrotic and apoptotic-like cells after (b) 6 h, (c) 24 h, and (d) 48 h of treatment. The control was 0.1% DMSO. Scale, 10 μm. *, statistically significant differences relative to the control and between treatments ($P < 0.001$) were determined by ANOVA with Student-Newman-Keuls multiple-comparison test.

membrane potential (71), wherein mitochondrial dysfunction and mitochondrial permeability transition induction are candidate intermediate steps in cell death (71, 72).

Oxidative membrane alterations can result in a secondary intracellular Ca^{2+} increase responsible for the irreversible disruption of membrane continuity (72). Calcium homeostasis is crucial for the correct functioning of mitochondria, and many antileishmanial agents exert their cytotoxic effects through the disruption of Ca^{2+} homeostasis in the parasite (49, 64). Ca^{2+} is stored in the acidocalcisomes, the ER, and the mitochondrion in trypanosomatids, keeping the cytosolic Ca^{2+} constant. Disruption of cytosolic Ca^{2+} signaling (73) and mitochondrial Ca^{2+} (73) may cause the parasite's death or interfere with its virulence. Ca^{2+} transport mechanisms common to eukaryotic cells operate in the mitochondria of trypanosomatid parasites, such as the mitochondrial calcium uniporter (MCU), the voltage-dependent anion channel (VDAC1), and the Ca^{2+}/H^{+} exchanger (CHX) (73, 74). VDAC1 in the outer mitochondrial membrane permits the Ca^{2+} influx into the intermembrane space and MCU in the inner mitochondrial membrane transport Ca^{2+} ions into the inner mitochondrial space (75). Efflux of Ca^{2+} to the cytosol from the inner mitochondrial space occurs via the Ca^{2+}/H^{+} exchanger. The transport of Ca^{2+} into the mitochondria is membrane potential-dependent, and

compounds that perturb the mitochondrial membrane potential result in Ca^{2+} release from the mitochondria into the cytosol as observed for FCCP. We demonstrated that promastigotes treated with CP2 suffer a loss of mitochondrial membrane potential and release of mitochondrial Ca^{2+} into the cytosol. Our results demonstrated that the high levels of $[Ca^{2+}]_i$ observed in *Leishmania* exposed to CP2 were derived from the mitochondrion as a result of the loss of mitochondrial membrane potential.

Increased *Leishmania* calreticulin and PDI levels after CP2 exposure were also observed. Calreticulin is a protein that presents high affinity for Ca^{2+}, contributing to the maintenance of Ca^{2+} homeostasis. However, its Ca^{2+} affinity decreases in the presence of PDI (76), leading to a rapid disturbance in its homeostasis, which can be translated into cell death processes (77, 78).

The cyclopalladated compound DPPE 1.1, and not Pd^{2+}, induced mitochondrial permeabilization and elevation in the cytosolic Ca^{2+} levels from intracellular pools, since $PdCl_2$ was not able to promote the same effect on the cation permeabilization (47). Similarly, the heavy metal ion chelator TPEN used here could not prevent the CP2-induced cytosolic Ca^{2+} increase, suggesting that the observed effect was not due to free Pd^{2+}. Additionally, the [Pd(C^2,*N*-dmba)(N_3)] CP2's moiety is important for the Ca^{2+} to unbalance, since free dmba did not exert an antileishmanial effect (29).

Protein folding is sensitive to changes in Ca^{2+} flux and the parasite's exposure to reducing agents (79). Proteins such as HSP70, HSP10, GRP78, and PDI play an important role in repairing the correct three-dimensional structure of unfolded proteins or forming aggregates due to stress. The observed increment of these proteins in CP2-treated parasites suggests the parasite's efforts to refold proteins and diminish the harmful effect of CP2 to the cell. Moreover, GRP78, HSP70, and PDI are dependent on ATPase activity (80) and are strongly related to the increase in proteins secreted inside ER and degraded by the proteasome. The above-mentioned findings will be the subject of analysis in future studies.

In trypanosomatids, apoptosis-like cell death mechanisms associated with a lack of molecular markers and conditions are not fully understood (81). It is known that low ROS levels promote apoptosis events, while necrosis is observed at high ROS levels (72, 82–84). Our data showed that *Leishmania* exposed to CP2 increased ROS levels for 60 min, which favored the necrotic process as seen in parasites exposed to CP2 for 24 h. Moreover, the percentage of living or apoptotic-like promastigotes after CP2 exposure increased in the presence of NAC. Indeed, our previous work (30) reported an inflammatory process in a *L. amazonensis*-infected BALB/c mice treated with CP2, which might corroborate the high number of necrotic cells detected after parasite exposure to CP2 for 48 h.

It is important to consider that Ca^{2+} also plays an important role in cell death mechanisms inducing both apoptosis (low Ca^{2+} levels) or necrosis (high Ca^{2+} levels) (72, 82, 84). We have shown here that promastigotes exposed to CP2 displayed changes in $[Ca^{2+}]_i$, followed by cell death. Thus, high ROS and $[Ca^{2+}]_i$ levels were observed ~10 min after CP2 addition, which suggested that ROS production is shortly followed by release of mitochondrial Ca^{2+}. These data suggest that ROS might be playing an essential role in the signaling/execution of the observed cell death mechanism and that Ca^{2+} acts on the observed mitochondrial changes, such as membrane depolarization, pointing out the parasite mitochondrion as central in orchestrating cell fate after triggering cell death signaling induced by CP2 (34, 49, 85).

Finally, beyond the previously reported antileishmanial efficacy of CP2 in a CL mouse model (30), here, we demonstrated that CP2 is also able to diminish the parasite load in a hamster model, as a visceral leishmaniasis model, indicating the broad potential of CP2 to exert its antileishmanial activity targeting other leishmaniasis clinical manifestations. Thus, the work presented here will help to promote rational drug modifications and thus contribute to the pipeline of leishmaniasis drug discovery.

MATERIALS AND METHODS

Compounds. The binuclear cyclopalladated complex [Pd(C^2,*N*-dmba)(μ-N_3)]$_2$ (dmba, N,N-dimethylbenzylamine), here called CP2, was obtained as previously described (86). Stock solutions of CP2,

amphotericin B (AmpB; Cristalia, São Paulo, Brazil), nigericin (Sigma-Aldrich), FCCP (Sigma-Aldrich), ionomycin (Sigma-Aldrich), CPA (Calbiochem, San Diego, CA), and TPEN (Sigma-Aldrich) were dissolved in dimethyl sulfoxide (DMSO) (Sigma-Aldrich) and further diluted in culture medium (final 0.1% DMSO). Stock solutions were kept at −20°C.

Biological assay. (i) Parasite culture. Promastigotes of *L. mexicana* strain MNYC/BZ/62/M379 and *L. infantum* strain MHOM/BR/1972/LD were maintained in Schneider's insect medium (Sigma-Aldrich), and *L. amazonensis* strain MPRO/BR/1972/M1841-LV-79 was maintained in liver-infusion tryptose (LIT) medium (87) at 28°C, supplemented with 10% heat-inactivated bovine serum (iFBS; Gibco/Invitrogen) and 1% penicillin/streptomycin (Sigma-Aldrich).

(ii) Animals. Male Swiss albino mice used to evaluate *in vitro* leishmanicidal activity against intracellular amastigotes were obtained from São Paulo State University (UNESP, Araraquara, São Paulo, Brazil). Male golden hamsters (*Mesocricetus auratus*) used in *in vivo* assays were acquired from ANILAB (Animais de Laboratório Criação e Comércio Ltda., Paulínia, São Paulo, Brazil). All animals were maintained in single-sex cages under a 12-h light/12-h dark cycle in a controlled-temperature room (22 ± 2°C), and they were fed *ad libitum*. The Ethics Committee for Animal Experimentation of São Paulo State University (UNESP), School of Pharmaceutical Sciences (CEUA/FCF/CAr, 18/2015 and 44/2015) approved this study in agreement with the guidelines of Sociedade Brasileira de Ciência de Animais de Laboratório (SBCAL) and Conselho Nacional de Controle da Experimentação Animal (CONCEA).

Antileishmanial *in vivo* assay. To analyze the potential spectrum of action of CP2, we evaluated *in vitro* and *in vivo* leishmanicidal activity of the cyclopalladated complex against *L. infantum*. The MTT [3-(4,5-dimethyl-2-thiazolyl)-2,5-diphenyl-2H-tetrazolium bromide] assay evaluated the susceptibility of *L. infantum* promastigotes, and evaluation of intracellular amastigotes forms was done according to a previously reported methodology (29, 30), followed by evaluation of *in vivo* leishmanicidal activity of CP2 against *L. infantum*-infected hamsters according to a previously established methodology (88). Briefly, 8-week-old male golden hamsters were intraperitoneally infected with 2×10^8 promastigotes of *L. infantum* in the stationary phase of growth and randomly separated into six groups containing five animals per cage. Then, 75 days postinfection, the animals received 15 daily intraperitoneal doses of CP2 (1.5 or 0.75 mg/kg/day), the reference drug AmpB (20 mg/kg/day), or phosphate-buffered saline (PBS) (vehicle); untreated infected animals and noninfected animals were also evaluated. The animals were euthanized at the end of treatment. According to a previously established methodology, the blood was collected by cardiac puncture to obtain blood serum samples to analyze liver and renal function biomarkers (88). Parasite burden in the spleen and liver was determined by the limiting dilution methodology as previously described (88, 89).

Proteomic analyses. For comparative proteomic analysis, 1×10^7 parasites ml^{-1} of promastigote forms of *L. amazonensis* in the mid-log phase were treated with 13.3 μmol liter^{-1} CP2 (IC_{50} of CP2 previously reported) (30) for 72 h. The extraction of total proteins of promastigotes was carried out in the presence (treated cells) and absence of CP2 (untreated cells). The parasite cultures were made in biological triplicates.

Protein extraction. Promastigote forms of *L. amazonensis* untreated and treated with CP2 were centrifuged at 2,000 × *g* for 10 min at 4°C. The pellet was washed three times with tryps wash (100 mmol liter^{-1} NaCl, 3 mmol liter^{-1} $MgCl_2$, and 20 mmol liter^{-1} Tris-HCl, pH 7.5) and resuspended in 500 μl of lysis solution (7 mol liter^{-1} urea, 2 mol liter^{-1} thiourea, 4% CHAPS, 2% IPG buffer 3-10, and 40 mmol liter^{-1} DTT) (90) containing a protease inhibitor cocktail (cOmplete, mini-protease inhibitor cocktail; Roche) for 1 h under constant stirring at 4°C. Finally, the supernatant was collected by centrifugation at 14,000 × *g* for 3 min at 4°C and stored at −80°C until the time of use. Protein extract quantification was performed with the 2D Quant kit (GE Healthcare) using the Infinite 200 PRO plate reader (Tecan).

Two-dimensional SDS-PAGE. Two-dimensional (2D) gels were run in triplicate according to standard procedures. pH 4 to 7 IPG buffer (Sigma-Aldrich) and bromophenol blue were added to 61.5 μg of protein and run on 24- cm pH 4 to 7 strips (GE Healthcare). The strips were equilibrated in equilibration buffer (6 mol liter^{-1} urea, 75 mmol liter^{-1} Tris-HCl, pH 8.8, 29.3% glycerol, 2% SDS, and 0.002% bromophenol blue) containing 25 mg ml^{-1} dithiothreitol (DTT) for 15 min under gentle stirring. The previous solution was discarded, and a new equilibration buffer containing 10 mg ml^{-1} iodoacetamide was added for 15 min. For the first dimension, rehydrated strips containing protein extracts of *L. amazonensis* promastigotes were transferred to ceramic support (Ettan IPGphor Manifold; GE Healthcare) and subjected to 50 μA per strip for protein migration using the Ettan IPGphor II isoelectric focusing system (GE Healthcare). The second dimension was run on 12.5% polyacrylamide gels (40 mA per gel) under continuous cooling (10°C) using an SE 600 Ruby and Multitemp IV instrument (GE Healthcare). The gels were stained with 0.1% Phast gel blue R solution (GE Healthcare) before scanning and analysis using ImageMaster 2D Platinum 7.0 software (GE Healthcare). Spots were cut, destained, and dried before trypsinization. Briefly, the spots were washed three times using 0.1 mol liter^{-1} NH_4HCO_3 in 50% acetonitrile (ACN), followed by the addition of pure ACN for 15 min. Finally, the spots were air-dried and trypsinized with Trypsin Gold mass spectrometry grade (Promega) according to the manufacturer's instructions.

Mass spectrometry (MS) analysis. The analysis of tryptic peptides was performed with a nanoACQUITY UPLC device (Waters, Milliford, MA, USA) coupled to the mass spectrometer Xevo Q-TOF G2 (Waters). For this, the UPLC nanoACQUITY system was equipped with a column of high-strength silica (HSS) T3 (Acquity UPLC HSS T3 column 75 mm by 150 mm; 1.8 μm; Waters), previously equilibrated with 7% of the mobile phase B (100% ACN + 0.1% formic acid). The peptides were separated by a linear gradient of 7% to 85% of mobile phase B for 20 min with 0.35 μl min^{-1} of flow at 45°C. The MS was operated in positive ion mode, with a data acquisition time of 20 min. The data obtained were processed using ProteinLynx GlobalServer 3.0 software (PLGS) (Waters). Protein identification of *L. amazonensis* was performed using the ion count algorithm

integrated with the software and searched against the *Leishmania mexicana* UniProt (Universal Protein Resource, http://www.uniprot.org/proteomes/?query=Leishmania&sort=score, proteome ID UP000007259) protein database (analysis date, March 2016), used for comparison purposes since *L. amazonensis* and *L. mexicana* are phylogenetically related (6, 7, 91).

Cell cycle analysis. Promastigotes of *L. amazonensis* were grown in an LIT medium at 28°C. Parasites in the exponential phase of growth (3×10^6 parasites ml^{-1}) were incubated with 5 mmol liter^{-1} hydroxyurea (HU) for 8 h and then transferred to HU-free medium supplemented with 0.03% DMSO, 20 μmol liter^{-1} NAC (*N*-acetyl-L-cysteine; Sigma), 53.2 or 133 μmol liter^{-1} CP2 (4× IC_{50} or 10× IC_{50}), and 20 μmol liter^{-1} NAC + 53.2 or 133 μmol liter^{-1} CP2. Cells were collected after 2, 4, 6, or 8 h of treatment, washed with 1× PBS, and fixed in 30% PBS/70% methanol overnight at 4°C. Fixed cells were washed with 1× PBS and stained with PBS solution containing propidium iodide (10 μg ml^{-1}) and RNase A (10 μg ml^{-1}) at 37°C for 30 min. Flow cytometry data were collected using the BD FACSCanto 1 flow cytometer. Data were analyzed using FlowJo software.

Intracellular ROS measurement. Intracellular ROS levels were compared after *L. amazonensis* exposure to CP2 based on the methodology previously described with some modifications (92). Briefly, parasites cultivated in Schneider's insect medium until the mid-log growth phase were harvested, washed, and resuspended in modified 1 Hanks' Balanced Salts (HBSS; Sigma) medium containing 1.3 mmol liter^{-1} $CaCl_2$. Then, 1×10^7 promastigotes ml^{-1} were incubated in the dark with 20 mmol liter^{-1} H_2DCFDA (2′,7′-dichlorodihydrofluorescein diacetate; Sigma) for 30 min, followed by treatment with different concentrations of CP2 based on the previously determined IC_{50} value as follows (30): 6.7 μmol liter^{-1} (0.5× IC_{50}), 13.3 μmol liter^{-1} (1× IC_{50}), 26.6 μmol liter^{-1} (2× IC_{50}), and 53.2 μmol liter^{-1} (4× IC_{50}). A volume of 200 μl of parasites was transferred to the wells of black-bottom plates, and the fluorescence was measured at 530 nm (emission) and 480 nm (excitation) for 60 min (Infinite 200; Tecan), and the basal fluorescence was subtracted at the end of the process.

Live-cell Fura-2 Ca^{2+} imaging. Promastigotes of *L. mexicana* in the mid-log phase (1×10^7 parasites ml^{-1}) were harvested and subsequently washed in loading buffer (8.5 mmol liter^{-1} Na_2HPO_4, 1.5 mmol liter^{-1} KH_2PO_4, 137 mmol liter^{-1} NaCl, 4 mmol liter^{-1} KCl, 10 mmol liter^{-1} HEPES 0.8 mmol liter^{-1} $MgCl_2$, 0.8 mmol liter^{-1} $MgSO_4$, 5 mmol liter^{-1} glucose, and 2.4 mmol liter^{-1} probenecid, pH 7.4), with and without 1.3 mmol liter^{-1} $CaCl_2$, which contained 5 μmol liter^{-1} Fura-2/AM (2-{6-[bis(carboxymethyl)amino]-5-(2-{2-[bis(carboxymethyl)amino]-5-methylphenoxy}ethoxy)-1-benzofuran-2-yl}-1,3-oxazole-5-carboxylic acid; Molecular Probes, Eugene, OR) and 2 μmol liter^{-1} pluronic acid F-127 (Molecular Probes). The suspensions were incubated for 2 h at 28°C in the dark. Parasites were washed twice with the loading buffer to remove the extracellular dye and immobilized on coverslips previously treated with 2 μl Cell Tak (Cell-Tak cell and tissue adhesive; Corning) for 5 min. The coverslip containing the immobilized cells was transferred to the microscope stage (thermostatically regulated microscope chamber, open perfusion microincubator [PDMI-2]) at 28°C. The fluorescence of promastigote forms loaded with Fura-2/AM was captured at ×40 magnification, using an inverted microscope (Eclipse TE300; Nikon, Melville, NY) coupled to a digital camera (Hamamatsu EM-CCD ImagEM). Image acquisition was performed every 3 s at 340 nm and 380 nm excitation and 510 nm emission. A series of images generated in-frame was transformed into a video with the software NIS-Elements AR 4.20.02. The results were obtained from at least three independent experiments of 100 promastigote forms per assay. Responses to the addition of different compounds were captured in real time, followed by 10 μmol liter^{-1} ionomycin to determine maximal fluorescence.

Measurement of the mitochondrial transmembrane potential $\Delta\psi_m$. Changes in the $\Delta\psi_m$ were measured spectrofluorimetrically using the cationic lipophilic dye 5,5′,6,6′-tetrachloro-1,1′,3,3′-tetraethylbenzimidazole carbocyanide iodide (JC-1; Sigma-Aldrich). Briefly, 2×10^6 promastigotes ml^{-1} of *L. amazonensis* were cultured for 60 min in the presence or absence of CP2. The parasites were harvested, resuspended in HBSS containing 1.3 mmol liter^{-1} $CaCl_2$, and incubated with JC-1 (10 μmol liter^{-1}) for 10 min at 28°C. For the positive control, 50 μmol liter^{-1} of the mitochondrial uncoupler carbonyl cyanide 3-chlorophenylhydrazone (CCCP) was added to untreated control cells 15 min before addition of JC-1. After washing twice with HBSS, fluorescence was measured at 530 nm and 590 nm using a spectrofluorometer (Tecan) with an excitation wavelength of 485 nm. The 590 nm/530 nm ratio values were plotted as the relative $\Delta\psi_m$ (93).

Cell death analysis using acridine orange/ethidium bromide (AO/EB) staining. Promastigotes of *L. amazonensis* in the mid-log phase (1×10^7 parasites ml^{-1}) were incubated with 13.3 μmol liter^{-1} CP2 for 6 h, 24 h, and 48 h. Likewise, parasites were incubated with 0.1% DMSO as a control. In addition, parasites were pretreated with 20 μmol liter^{-1} NAC for 2 h before CP2 addition. After the incubation period, the parasites were centrifuged for 10 min at 2,000 × *g*, washed with PBS, and resuspended in 200 μl of PBS. Then, 20 μl of cell suspension was stained with a mixture of ethidium bromide and acridine orange (100 μg ml^{-1}) and immobilized on a glass coverslip previously treated with Cell Tak, as described above. The labeled parasites were visualized by fluorescence microscopy (Axioplan-Zeiss) with ×100 magnification and a fluorescein isothiocyanate (FITC) filter (460 to 490 nm band-pass excitation filter and 510 to 560 nm emission) according to a previously described methodology (57). For the percentage quantification of each event, 200 cells from each sample were counted.

Statistical analysis. The biological assays' data were analyzed by one-way analysis of variance (ANOVA) followed by Tukey and Student-Newman-Keuls multiple-comparison tests (Graph Pad InStat software and GraphPad Prism software). Differences were considered significant when P was ≤ 0.05.

ACKNOWLEDGMENTS

This work was supported by the São Paulo Research Foundation (FAPESP) grants 2016/05345-4, 2016/177115, 2017/03552-5, 2018/23015-7, and 2020/04415-4; Programa

de Apoio ao Desenvolvimento Científico da Faculdade de Ciências Farmacêuticas da UNESP (PADC); and funding from the Thomas P. Infusino Endowment at Rutgers University. A.M.A.V. (2016/19289-9 and 2019/21661-1) and S.V. (2016/18191-5) were supported by FAPESP. This study was financed in part by the Coordenação de Aperfeiçoamento de Pessoal de Nível Superior-Brasil (CAPES)-finance code 001 (I.A.P.L., T.G.P., K.B.I., and J.M.V.). M.A.R.B., A.V.G.N., and M.A.S.G. are recipients of a Research Productivity Scholarship from the National Council for Research and Development (CNPq).

We thank Janice Rodrigues Perussi, USP-São Carlos, for kindly allowing us to have access to the fluorescence microscope, and "Núcleo de atendimento à comunidade (NAC), FCF, UNESP," for the analysis of biomarkers of liver and renal function. The funders had no role in study design, data collection, analysis, decision to publish, or manuscript preparation.

A.M.A.V., L.R.O.T., A.P.T., and M.A.S.G. designed the studies. J.M.V. and A.V.G.N. synthesized the cyclopalladated complex CP2. A.M.A.V., I.A.P.L., T.G.P., D.D.L.T., K.B.I., S.V., and A.D.L.L. performed the experiments and acquired the data. A.M.A.V., P.J.B., I.A.P.L., T.G.P., D.D.L.T., K.B.I., S.V., L.R.O.T., M.A.R.B., A.V.G.N., A.P.T., and M.A.S.G. contributed to the data analysis and interpretation results. A.M.A.V. wrote the manuscript. A.M.A.V., P.J.B., L.R.O.T., M.A.R.B., A.P.T., and M.A.S.G. reviewed and edited the manuscript.

We declare no conflict of interest.

REFERENCES

1. Burza S, Croft SL, Boelaert M. 2018. Leishmaniasis. Lancet 392:951–970. https://doi.org/10.1016/S0140-6736(18)31204-2.
2. Barrett MP, Croft SL. 2012. Management of trypanosomiasis and leishmaniasis. Br Med Bull 104:175–196. https://doi.org/10.1093/bmb/lds031.
3. Lindoso JAL, Cunha MA, Queiroz IT, Moreira CHV. 2016. Leishmaniasis-HIV coinfection: current challenges. HIV AIDS (Auckl) 8:147–156. https://doi.org/10.2147/HIV.S93789.
4. Monzote L. 2009. Current treatment of leishmaniasis: a review. Open Antimicrob Agents J 1:9–19.
5. Herwaldt BL. 1999. Leishmaniasis. Lancet 354:1191–1199. https://doi.org/10.1016/S0140-6736(98)10178-2.
6. Silveira FT, Lainson R, Corbett CEP. 2004. Clinical and immunopathological spectrum of American cutaneous leishmaniasis with special reference to the disease in Amazonian Brazil: a review. Mem Inst Oswaldo Cruz 99:239–251. https://doi.org/10.1590/s0074-02762004000300001.
7. Mann S, Frasca K, Scherrer S, Henao-Martínez AF, Newman S, Ramanan P, Suarez JA. 2021. A review of leishmaniasis: current knowledge and future directions. Curr Trop Med Rep 8:121–132. https://doi.org/10.1007/s40475-021-00232-7.
8. Singh N, Kumar M, Singh RK. 2012. Leishmaniasis: current status of available drugs and new potential drug targets. Asian Pac J Trop Med 5:485–497. https://doi.org/10.1016/S1995-7645(12)60084-4.
9. Van Griensven J, Diro E. 2012. Visceral leishmaniasis. Infect Dis Clin North Am 26:309–322. https://doi.org/10.1016/j.idc.2012.03.005.
10. Croft SL, Sundar S, Fairlamb AH. 2006. Drug resistance in leishmaniasis. Clin Microbiol Rev 19:111–126. https://doi.org/10.1128/CMR.19.1.111-126.2006.
11. Meheus F, Balasegaram M, Olliaro P, Sundar S, Rijal S, Faiz MA, Boelaert M. 2010. Cost-effectiveness analysis of combination therapies for visceral leishmaniasis in the Indian subcontinent. PLoS Negl Trop Dis 4:e818. https://doi.org/10.1371/journal.pntd.0000818.
12. Palumbo E. 2009. Current treatment for cutaneous leishmaniasis: a review. Am J Ther 16:178–182. https://doi.org/10.1097/MJT.0b013e3181822e90.
13. Katsuno K, Burrows JN, Duncan K, van Huijsduijnen RH, Kaneko T, Kita K, Mowbray CE, Schmatz D, Warner P, Slingsby BT. 2015. Hit and lead criteria in drug discovery for infectious diseases of the developing world. Nat Rev Drug Discov 14:751–758. https://doi.org/10.1038/nrd4683.
14. Chawla B, Madhubala R. 2010. Drug targets in Leishmania. J Parasit Dis 34:1–13. https://doi.org/10.1007/s12639-010-0006-3.
15. Siqueira-Neto JL, Song O-R, Oh H, Sohn J-H, Yang G, Nam J, Jang J, Cechetto J, Lee CB, Moon S, Genovesio A, Chatelain E, Christophe T, Freitas-Junior LH. 2010. Antileishmanial high-throughput drug screening reveals drug candidates with new scaffolds. PLoS Negl Trop Dis 4:e675. https://doi.org/10.1371/journal.pntd.0000675.
16. Freitas-Junior LH, Chatelain E, Kim HA, Siqueira-Neto JL. 2012. Visceral leishmaniasis treatment: what do we have, what do we need and how to deliver it? Int J Parasitol Drugs Drug Resist 2:11–19. https://doi.org/10.1016/j.ijpddr.2012.01.003.
17. Akbari M, Oryan A, Hatam G. 2017. Application of nanotechnology in treatment of leishmaniasis: a review. Acta Trop 172:86–90. https://doi.org/10.1016/j.actatropica.2017.04.029.
18. De Almeida L, Fujimura AT, Del Cistia ML, Fonseca-Santos B, Imamura KB, Michels PAM, Chorilli M, Graminha MAS. 2017. Nanotechnological strategies for treatment of leishmaniasis: a review. J Biomed Nanotechnol 13:117–133. https://doi.org/10.1166/jbn.2017.2349.
19. Torres FAE, Passalacqua TG, Velásquez AMA, de Souza RA, Colepicolo P, Graminha MAS. 2014. New drugs with antiprotozoal activity from marine algae: a review. Brazilian J Pharmacogn 24:265–276. https://doi.org/10.1016/j.bjp.2014.07.001.
20. Falkenberg M, Nakano E, Zambotti-Villela L, Zatelli GA, Philippus AC, Imamura KB, Velasquez AMA, Freitas RP, Tallarico LDF, Colepicolo P, Graminha MAS. 2019. Bioactive compounds against neglected diseases isolated from macroalgae: a review. J Appl Phycol 31:797–823. https://doi.org/10.1007/s10811-018-1572-5.
21. Elgazwy A-SSH, Ismail NSM, Atta-Allah SR, Sarg MT, Soliman DHS, Zaki MY, Elgamas MA. 2012. Palladacycles as antimicrobial agents. Curr Med Chem 19:3967–3981. https://doi.org/10.2174/092986712802002527.
22. Anilanmert B. 2012. Therapeutic organometallic compounds, p 651–680. *In* Galleli L (ed), Pharmacology. IntechOpen, Istanbul University, Institute of Forensic Sciences, Istanbul, Turkey.
23. Farrell N. 2003. Metal complexes as drugs and chemotherapeutic agents, p 809–840. *In* McCleverty JA, Meyer TJ, Comprehensive Coordination Chemistry II. Elsevier, Amsterdam, The Netherlands.
24. Sánchez-Delgado RA, Anzellotti A. 2004. Metal complexes as chemotherapeutic agents against tropical diseases: trypanosomiasis, malaria and leishmaniasis. Mini-Rev Med Chem 4:23–30. https://doi.org/10.2174/1389557043487493.
25. Fricker SP, Mosi RM, Cameron BR, Baird I, Zhu Y, Anastassov V, Cox J, Doyle PS, Hansell E, Lau G, Langille J, Olsen M, Qin L, Skerlj R, Wong RSY, Santucci Z, McKerrow JH. 2008. Metal compounds for the treatment of parasitic diseases. J Inorg Biochem 102:1839–1845. https://doi.org/10.1016/j.jinorgbio.2008.05.010.
26. Navarro M, Gabbiani C, Messori L, Gambino D. 2010. Metal-based drugs for malaria, trypanosomiasis and leishmaniasis: recent achievements and

perspectives. Drug Discov Today 15:1070–1078. https://doi.org/10.1016/j.drudis.2010.10.005.
27. Lopera AA, Velásquez AMA, Clementino LC, Robledo S, Montoya A, de Freitas LM, Bezzon VDN, Fontana CR, Garcia C, Graminha MAS. 2018. Solution-combustion synthesis of doped TiO2 compounds and its potential antileishmanial activity mediated by photodynamic therapy. J Photochem Photobiol B Biol 183:64–74. https://doi.org/10.1016/j.jphotobiol.2018.04.017.
28. Velásquez AMA, Francisco AI, Kohatsu AAN, de Silva FAJ, Rodrigues DF, da Silva Teixeira RG, Chiari BG, de Almeida MGJ, Isaac VLB, Vargas MD, Cicarelli RMB. 2014. Synthesis and tripanocidal activity of ferrocenyl and benzyl diamines against Trypanosoma brucei and Trypanosoma cruzi. Bioorg Med Chem Lett 24:1707–1710. https://doi.org/10.1016/j.bmcl.2014.02.046.
29. Velásquez AMA, de Souza RA, Passalacqua TG, Ribeiro AR, Scontri M, Chin CM, de Almeida L, Del Cistia ML, da Rosa JA, Mauro AE, Graminha MAS. 2016. Antiprotozoal activity of the cyclopalladated complexes against Leishmania amazonensis and Trypanosoma cruzi. J Braz Chem Soc 27:1032–1039. https://doi.org/10.5935/0103-5053.20150360.
30. Velásquez AMA, Ribeiro WC, Venn V, Castelli S, de Camargo MS, de Assis RP, de Souza RA, Ribeiro AR, Passalacqua TG, da Rosa JA, Baviera AM, Mauro AE, Desideri A, Almeida-Amaral EE, Graminha MAS. 2017. Efficacy of a binuclear cyclopalladated compound therapy for cutaneous leishmaniasis in the murine model of infection with Leishmania amazonensis and its inhibitory effect on topoisomerase 1B. Antimicrob Agents Chemother 61:e00688-17. https://doi.org/10.1128/AAC.00688-17.
31. Clementino L da C, Velásquez AMA, Passalacqua TG, de Almeida L, Graminha MAS, Martins GZ, Salgueiro L, Cavaleiro C, do Sousa MC, Moreira RRD. 2018. In vitro activities of glycoalkaloids from the Solanum lycocarpum against Leishmania infantum. Brazilian J Pharmacogn 28:673–677. https://doi.org/10.1016/j.bjp.2018.07.008.
32. Passalacqua TG, Dutra LA, de Almeida L, Velásquez AMA, Torres FAE, Yamasaki PR, dos Santos MB, Regasini LO, Michels PAM, da Bolzani VS, Graminha MAS. 2015. Synthesis and evaluation of novel prenylated chalcone derivatives as anti-leishmanial and anti-trypanosomal compounds. Bioorg Med Chem Lett 25:3342–3345. https://doi.org/10.1016/j.bmcl.2015.05.072.
33. Matsuo AL, Silva LS, Torrecilhas AC, Pascoalino BS, Ramos TC, Rodrigues EG, Schenkman S, Caires ACF, Travassos LR. 2010. In vitro and in vivo trypanocidal effects of the cyclopalladated compound 7a, a drug candidate for treatment of Chagas' disease. Antimicrob Agents Chemother 54:3318–3325. https://doi.org/10.1128/AAC.00323-10.
34. Arruda DC, Matsuo AL, Silva LS, Real F, Leitão NP, Pires JHS, Caires ACF, Garcia DM, Cunha FFM, Puccia R, Longo LVG. 2015. Cyclopalladated compound 7a induces apoptosis- and autophagy-like mechanisms in paracoccidioides and is a candidate for paracoccidioidomycosis treatment. Antimicrob Agents Chemother 59:7214–7223. https://doi.org/10.1128/AAC.00512-15.
35. Paladi CDS, Pimentel IAS, Katz S, Cunha RLOR, de Judice WAS, Caires ACF, Barbiéri CL. 2012. In vitro and in vivo activity of a palladacycle complex on Leishmania (Leishmania) amazonensis. PLoS Negl Trop Dis 6:e1626. https://doi.org/10.1371/journal.pntd.0001626.
36. Paladi CS, da Silva DAM, Motta PD, Garcia DM, Teixeira D, Longo-Maugéri IM, Katz S, Barbiéri CL. 2017. Treatment of Leishmania (Leishmania) amazonensis-infected mice with a combination of a palladacycle complex and heat-killed propionibacterium acnes triggers protective cellular immune responses. Front Microbiol 8:1–11. https://doi.org/10.3389/fmicb.2017.00333.
37. Dos Santos IB, da Silva DAM, Paz FACR, Garcia DM, Carmona AK, Teixeira D, Longo-Maugéri IM, Katz S, Barbiéri CL. 2018. Leishmanicidal and immunomodulatory activities of the palladacycle complex DPPE 1.1, a potential candidate for treatment of cutaneous leishmaniasis. Front Microbiol 9:1–9. https://doi.org/10.3389/fmicb.2018.01427.
38. Vieites M, Otero L, Santos D, Toloza J, Figueroa R, Norambuena E, Olea-Azar C, Aguirre G, Cerecetto H, González M, Morello A, Maya JD, Garat B, Gambino D. 2008. Platinum(II) metal complexes as potential anti-Trypanosoma cruzi agents. J Inorg Biochem 102:1033–1043. https://doi.org/10.1016/j.jinorgbio.2007.12.005.
39. Navarro M, Hernández C, Colmenares I, Hernández P, Fernández M, Sierraalta A, Marchán E. 2007. Synthesis and characterization of [Au(dppz)2]Cl3. DNA interaction studies and biological activity against Leishmania (L) mexicana. J Inorg Biochem 101:111–116. https://doi.org/10.1016/j.jinorgbio.2006.08.015.
40. Zinsstag J, Brun R, Craciunescu DG, Parrondo Iglesias E. 1991. In vitro activity of organometallic complexes of Ir, Pt and Rh on Trypanosoma b. gambiense, T. b. rhodesiense and T. b. brucei. Trop Med Parasitol 42:41–44.
41. Croft SL, Neal RA, Craciunescu DG, Certad-Fombona G. 1992. The activity of platinum, iridium and rhodium drug complexes against Leishmania donovani. Trop Med Parasitol 43:24–28.
42. Santos D, Parajón-Costa B, Rossi M, Caruso F, Benítez D, Varela J, Cerecetto H, González M, Gómez N, Caputto ME, Moglioni AG, Moltrasio GY, Finkielsztein LM, Gambino D. 2012. Activity on Trypanosoma cruzi, erythrocytes lysis and biologically relevant physicochemical properties of Pd(II) and Pt(II) complexes of thiosemicarbazones derived from 1-indanones. J Inorg Biochem 117:270–276. https://doi.org/10.1016/j.jinorgbio.2012.08.024.
43. Otero L, Vieites M, Boiani L, Denicola A, Rigol C, Opazo L, Olea-Azar C, Maya JD, Morello A, Krauth-Siegel RL, Piro OE, Castellano E, González M, Gambino D, Cerecetto H. 2006. Novel antitrypanosomal agents based on palladium nitrofurylthiosemicarbazone complexes: DNA and redox metabolism as potential therapeutic targets. J Med Chem 49:3322–3331. https://doi.org/10.1021/jm0512241.
44. Franco LP, de Góis EP, Codonho BS, Pavan ALR, de Oliveira Pereira I, Marques MJ, de Almeida ET. 2013. Palladium(II) imine ligands cyclometallated complexes with a potential leishmanicidal activity on Leishmania (L.) amazonensis. Med Chem Res 22:1049–1056. https://doi.org/10.1007/s00044-012-0095-x.
45. Bjelogrlić SK, Todorović TR, Kojić M, Senćanski M, Nikolić M, Višnjevac A, Araškov J, Miljković M, Muller CD, Filipović NR. 2019. Pd(II) complexes with N-heteroaromatic hydrazone ligands: anticancer activity, in silico and experimental target identification. J Inorg Biochem 199:110758. https://doi.org/10.1016/j.jinorgbio.2019.110758.
46. Navarro M, Betancourt A, Hernández C, Marchán E. 2008. Palladium polypyridyl complexes: synthesis, characterization, DNA interaction and biological activity on Leishmania (L.) mexicana. J Braz Chem Soc 19:1355–1360. https://doi.org/10.1590/S0103-50532008000700018.
47. Serrano FA, Matsuo AL, Monteforte PT, Bechara A, Smaili SS, Santana DP, Rodrigues T, Pereira FV, Silva LS, Machado J Jr, Santos EL, Pesquero JB, Martins RM, Travassos LR, Caires ACF, Rodrigues EG. 2011. A cyclopalladated complex interacts with mitochondrial membrane thiol-groups and induces the apoptotic intrinsic pathway in murine and cisplatin-resistant human tumor cells. BMC Cancer 11:1–16. https://doi.org/10.1186/1471-2407-11-296.
48. Mutlu O. 2014. In silico molecular modeling and docking studies on the leishmanial tryparedoxin peroxidase. Brazilian Arch Biol Technol an Int J 57:244–252. https://doi.org/10.1590/S1516-89132014000200013.
49. Corral MJ, Benito-Peña E, Jiménez-Antón MD, Cuevas L, Moreno-Bondi MC, Alunda JM. 2016. Allicin induces calcium and mitochondrial dysregulation causing necrotic death in Leishmania. PLoS Negl Trop Dis 10:e0004525. https://doi.org/10.1371/journal.pntd.0004525.
50. Docampo R, Vercesi AE, Huang G. 2014. Mitochondrial calcium transport in trypanosomes. Mol Biochem Parasitol 196:108–116. https://doi.org/10.1016/j.molbiopara.2014.09.001.
51. Sen N, Das BB, Ganguly A, Mukherjee T, Bandyopadhyay S, Majumder HK. 2004. Camptothecin-induced imbalance in intracellular cation homeostasis regulates programmed cell death in unicellular hemoflagellate Leishmania donovani. J Biol Chem 279:52366–52375. https://doi.org/10.1074/jbc.M406705200.
52. Kowaltowski AJ, Castilho RF, Vercesi AE. 2001. Mitochondrial permeability transition and oxidative stress. FEBS Lett 495:12–15. https://doi.org/10.1016/s0014-5793(01)02316-x.
53. Marchi B, Burlando B, Panfoli I, Viarengo A. 2000. Interference of heavy metal cations with fluorescent Ca2+ probes does not affect Ca2+ measurements in living cells. Cell Calcium 28:225–231. https://doi.org/10.1054/ceca.2000.0155.
54. Takahashi A, Camacho P, Lechleiter JD, Herman B. 1999. Measurement of intracellular calcium. Physiol Rev 79:1089–1125. https://doi.org/10.1152/physrev.1999.79.4.1089.
55. Docampo R, Scott DA, Vercesi AE, Moreno SNJ. 1995. Intracellular Ca2+ storage in acidocalcisomes of Trypanosoma cruzi. Biochem J 310:1005–1012. https://doi.org/10.1042/bj3101005.
56. Moncoq K, Trieber CA, Young HS. 2007. The molecular basis for cyclopiazonic acid inhibition of the sarcoplasmic reticulum calcium pump. J Biol Chem 282:9748–9757. https://doi.org/10.1074/jbc.M611653200.
57. Linares IAP, de Oliveira KT, Perussi JR. 2017. Chlorin derivatives sterically-prevented from self-aggregation with high antitumor activity for

photodynamic therapy. Dye Pigment 145:518–527. https://doi.org/10.1016/j.dyepig.2017.06.011.
58. Zuma AA, Mendes IC, Reignault LC, Elias MC, de Souza W, Machado CR, Motta MCM. 2014. How Trypanosoma cruzi handles cell cycle arrest promoted by camptothecin, a topoisomerase I inhibitor. Mol Biochem Parasitol 193:93–100. https://doi.org/10.1016/j.molbiopara.2014.02.001.
59. Prada CF, Álvarez-Velilla R, Balaña-Fouce R, Prieto C, Calvo-Álvarez E, Escudero-Martínez JM, Requena JM, Ordóñez C, Desideri A, Pérez-Pertejo Y, Reguera RM. 2013. Gimatecan and other camptothecin derivatives poison Leishmania DNA-topoisomerase IB leading to a strong leishmanicidal effect. Biochem Pharmacol 85:1433–1440. https://doi.org/10.1016/j.bcp.2013.02.024.
60. Reguera RM, Díaz-González R, Pérez-Pertejo Y, Balaña-Fouce R. 2008. Characterizing the bi-subunit type IB DNA topoisomerase of Leishmania parasites; a novel scenario for drug intervention in trypanosomatids. Curr Drug Targets 9:966–978. https://doi.org/10.2174/138945008786786118.
61. Figarella K, Uzcategui NL, Beck A, Schoenfeld C, Kubata BK, Lang F, Duszenko M. 2006. Prostaglandin induced programmed cell death in Trypanosoma brucei involves oxidative stress. Cell Death Differ 13:1802–1814. https://doi.org/10.1038/sj.cdd.4401862.
62. Edinger AL, Thompson CB. 2004. Death by design: apoptosis, necrosis and autophagy. Curr Opin Cell Biol 16:663–669. https://doi.org/10.1016/j.ceb.2004.09.011.
63. Santana DP, Faria PA, Paredes-Gamero EJ, Caires ACF, Nantes IL, Rodrigues T. 2009. Palladacycles catalyse the oxidation of critical thiols of the mitochondrial membrane proteins and lead to mitochondrial permeabilization and cytochrome c release associated with apoptosis. Biochem J 417:247–256. https://doi.org/10.1042/BJ20080972.
64. Vincent IM, Racine G, Légaré D, Ouellette M. 2015. Mitochondrial proteomics of antimony and miltefosine resistant Leishmania infantum. Proteomes 3:328–346. https://doi.org/10.3390/proteomes3040328.
65. Mishra J, Singh S. 2013. Miltefosine resistance in Leishmania donovani involves suppression of oxidative stress-induced programmed cell death. Exp Parasitol 135:397–406. https://doi.org/10.1016/j.exppara.2013.08.004.
66. Canuto GAB, Castilho-Martins EA, Tavares MFM, Rivas L, Barbas C, López-Gonzálvez Á. 2014. Multi-analytical platform metabolomic approach to study miltefosine mechanism of action and resistance in Leishmania. Anal Bioanal Chem 406:3459–3476. https://doi.org/10.1007/s00216-014-7772-1.
67. Müller S, Liebau E, Walter RD, Krauth-Siegel RL. 2003. Thiol-based redox metabolism of protozoan parasites. Trends Parasitol 19:320–328. https://doi.org/10.1016/S1471-4922(03)00141-7.
68. Krauth-Siegel RL, Comini MA. 2008. Redox control in trypanosomatids, parasitic protozoa with trypanothione-based thiol metabolism. Biochim Biophys Acta 1780:1236–1248. https://doi.org/10.1016/j.bbagen.2008.03.006.
69. Turrens JF. 2004. Oxidative stress and antioxidant defenses: a target for the treatment of diseases caused by parasitic protozoa. Mol Aspects Med 25:211–220. https://doi.org/10.1016/j.mam.2004.02.021.
70. Barr SD, Gedamu L. 2003. Role of peroxidoxins in Leishmania chagasi survival. Evidence of an enzymatic defense against nitrosative stress. J Biol Chem 278:10816–10823. https://doi.org/10.1074/jbc.M212990200.
71. Harder S, Bente M, Isermann K, Bruchhaus I. 2006. Expression of a mitochondrial peroxiredoxin prevents programmed cell death in Leishmania donovani. Eukaryot Cell 5:861–870. https://doi.org/10.1128/EC.5.5.861-870.2006.
72. Petit PX. 2002. Mitochondrial implication in cell death. *In* Lemasters JJ, Nieminen A-L. Mitochondria in pathogenesis. Kluwer Academic Publishers, New York, NY.
73. Docampo R, Huang G. 2015. Calcium signaling in trypanosomatid parasites. Cell Calcium 57:194–202. https://doi.org/10.1016/j.ceca.2014.10.015.
74. De Stefani D, Rizzuto R. 2014. Molecular control of mitochondrial calcium uptake. Biochem Biophys Res Commun 449:373–376. https://doi.org/10.1016/j.bbrc.2014.04.142.
75. Scarpelli PH, Pecenin MF, Garcia CRS. 2021. Intracellular Ca^{2+} signaling in protozoan parasites: an overview with a focus on mitochondria. Int J Mol Sci 22:469. https://doi.org/10.3390/ijms22010469.
76. Baksh S, Burns K, Andrin C, Michalak M. 1995. Interaction of calreticulin with protein disulfide isomerase. J Biol Chem 270:31338–31344. https://doi.org/10.1074/jbc.270.52.31338.
77. Groenendyk J, Lynch J, Michalak M. 2004. Calreticulin, Ca^{2+}, and calcineurin: signaling from the endoplasmic reticulum. Mol Cells 17:383–389.
78. Lim S, Chang W, Lee BK, Song H, Hong JH, Lee S, Song B-W, Kim H-J, Cha M-J, Jang Y, Chung N, Choi S-Y, Hwang K-C. 2008. Enhanced calreticulin expression promotes calcium-dependent apoptosis in postnatal cardiomyocytes. Mol Cells 25:390–396.
79. Dolai S, Adak S. 2014. Endoplasmic reticulum stress responses in Leishmania. Mol Biochem Parasitol 197:1–8. https://doi.org/10.1016/j.molbiopara.2014.09.002.
80. Mayer M, Kies U, Kammermeier R, Buchner J. 2000. BiP and PDI cooperate in the oxidative folding of antibodies in vitro. J Biol Chem 275:29421–29425. https://doi.org/10.1074/jbc.M002655200.
81. Kaczanowski S, Sajid M, Reece SE. 2011. Evolution of apoptosis-like programmed cell death in unicellular protozoan parasites. Parasit Vectors 4:44. https://doi.org/10.1186/1756-3305-4-44.
82. Lemasters JJ, Nieminen A-L, Qian T, Trost LC, Elmore SP, Nishimura Y, Crowe RA, Cascio WE, Bradham CA, Brenner DA, Herman B. 1998. The mitochondrial permeability transition in cell death: a common mechanism in necrosis, apoptosis and autophagy. Biochim Biophys Acta 1366:177–196. https://doi.org/10.1016/s0005-2728(98)00112-1.
83. Kim J-S, He L, Lemasters JJ. 2003. Mitochondrial permeability transition: a common pathway to necrosis and apoptosis. Biochem Biophys Res Commun 304:463–470. https://doi.org/10.1016/s0006-291x(03)00618-1.
84. Lemasters JJ, Theruvath TP, Zhong Z, Nieminen A-L. 2009. Mitochondrial calcium and the permeability transition in cell death. Biochim Biophys Acta 1787:1395–1401. https://doi.org/10.1016/j.bbabio.2009.06.009.
85. Tagliarino C, Pink JJ, Dubyak GR, Nieminen A-L, Boothman DA. 2001. Calcium is a key signaling molecule in beta-lapachone-mediated cell death. J Biol Chem 276:19150–19159. https://doi.org/10.1074/jbc.M100730200.
86. de Almeida ET, Mauro AE, Santana AM, Ananias SR, Godoy Netto AV, Ferreira JG, Santos RHA. 2007. Self-assembly of organometallic Pd(II) complexes via CH3$\cdots\pi$ interactions: the first example of a cyclopalladated compound with herringbone stacking pattern. Inorg Chem Commun (Camb) 10:1394–1398. https://doi.org/10.1016/j.inoche.2007.08.020.
87. Silva LHP, Nussenzweig V. 1953. Sobre uma cepa de Trypanosoma cruzi altamente virulenta para o camundongo branco. Folia Clin Biol 20:191–208.
88. de Almeida L, Passalacqua TG, Dutra LA, da Fonseca JNV, Nascimento RFQ, Imamura KB, de Andrade CR, dos Santos JL, Graminha MAS. 2017. In vivo antileishmanial activity and histopathological evaluation in Leishmania infantum infected hamsters after treatment with a furoxan derivative. Biomed Pharmacother 95:536–547. https://doi.org/10.1016/j.biopha.2017.08.096.
89. Lima HC, Bleyenberg JA, Titus RG. 1997. A simple method for quantifying Leishmania in tissues of infected animals. Parasitol Today 13:80–82. https://doi.org/10.1016/s0169-4758(96)40010-2.
90. Görg A. 2004. 2-D electrophoresis: principles and methods. Munich, Germany. https://rs.umc.edu.dz/umc/2_D_Electrophoresis.pdf.
91. Tschoeke DA, Nunes GL, Jardim R, Lima J, Dumaresq ASR, Gomes MR, Pereira LDM, Loureiro DR, Stoco PH, Leonel H, Guedes DM, De Miranda AB, Pitaluga A, da Silva FP Jr, Probst CM, Dickens NJ, Mottram JC, Grisard EC, Dávila AMR. 2014. The comparative genomics and phylogenomics of Leishmania amazonensis parasite. Evol Bioinforma 8:131–153. https://doi.org/10.4137/EBO.S13759.
92. Fonseca-Silva F, Inacio JDF, Canto-Cavalheiro MM, Almeida-Amaral EE. 2011. Reactive oxygen species production and mitochondrial dysfunction contribute to quercetin induced death in Leishmania amazonensis. PLoS One 6:e14666. https://doi.org/10.1371/journal.pone.0014666.
93. Mukherjee P, Majee SB, Ghosh S, Hazra B. 2009. Apoptosis-like death in Leishmania donovani promastigotes induced by diospyrin and its ethanolamine derivative. Int J Antimicrob Agents 34:596–601. https://doi.org/10.1016/j.ijantimicag.2009.08.007.